

Non-THC cannabinoids counteract prostate carcinoma growth in vitro and in vivo: pro-apoptotic effects and underlying mechanisms

Luciano De Petrocellis^{1*#}, Alessia Ligresti^{2*}, Aniello Schiano Moriello¹, Mariagrazia Iappelli¹, Roberta Verde², Colin G. Stott³, Luigia Cristino¹, Pierangelo Orlando^{4*} and Vincenzo Di Marzo^{2#}

^{1,2,4}Endocannabinoid Research Group, Consiglio Nazionale delle Ricerche, ¹Istituto di Cibernetica, ²Istituto di Chimica Biomolecolare and ⁴Istituto di Biochimica delle Proteine. ³GW Pharma Ltd., UK.

*These authors devoted equal experimental effort to this work

#Please address all correspondence to these authors at Endocannabinoid Research Group, Consiglio Nazionale delle Ricerche, Via Campi Flegrei 34, Comprensorio Olivetti, 80078, Pozzuoli (NA), Italy. Tel.: +39-081-8675093; fax: 081-8041770; e-mail: l.depetrocellis@cib.na.cnr.it or vdimarzo@icb.cnr.it

Running title: Cannabidiol and prostate carcinoma

Abbreviations: AR, Androgen receptor; BDS, Botanical drug substance; BRM, Botanical Raw Material; BSA, Bovine serum albumin; CB₁, Cannabinoid receptor 1; CB₂, Cannabinoid receptor 2; CBC, Cannabichromene; CBD, Cannabidiol; CBDA, Cannabidiolic acid; CBDV, Cannabidivarin; CBG, Cannabigerol; CBGA, Cannabigerolic acid; CBGV, Cannabigevarin; CBN, Cannabinol; CHOP, CCAAT/enhancer binding protein or DDIT3, DNA-damage-inducible transcript 3; Cq, Threshold cycles; Docetaxel, DCX; ER, Endoplasmic reticulum; ER α , Oestrogen receptor 1; ER β , Oestrogen receptor 2; FBS, Foetal bovine serum; GPER, G protein-coupled oestrogen receptor 1; MTT, 3-(4,5-Dimethylthiazol-2-yl)-2,5-diphenyltetrazolium bromide; NACWO, Named Animal Care and Welfare Officer; NGF, Nerve growth factor; NSE, neuron-specific enolase; NVS, Named Veterinary Surgeon; OMDM233, Phenyl-4-phenyl (-)-menthylamine; p21, Cyclin-dependent kinase inhibitor 1A; p27^{Kip}, Cyclin-dependent kinase inhibitor; p53, Tumor protein; PCC, Prostate carcinoma cell; PUMA, p53-upregulated modulator of apoptosis, BCL, binding component 3-BBC3; qRT-PCR, Quantitative Real Time-PCR; RNA pol, RNA polymerase II subunit; ROS, Reactive oxygen species; SDP, Serum deprived; TaOpt, Temperature-optimum-annealing; THC, Δ^9 -tetrahydrocannabinol; THCA, Δ^9 -tetrahydrocannabinolic acid; THCV, Δ^9 -tetrahydrocannabivarin; THCVA, Δ^9 -tetrahydrocannabivarinic acid; TRP, Transient receptor potential channel; TRPA1, Transient receptor potential

This article has been accepted for publication and undergone full scientific peer review but has not been through the copyediting, typesetting, pagination and proofreading process which may lead to differences between this version and the Version of Record. Please cite this article as an 'Accepted Article', doi: 10.1111/j.1476-5381.2012.02027.x

cation channel, subfamily A, member 1; TRPM8, Transient receptor potential cation channel, subfamily M, member 8; TRPV1, Transient receptor potential cation channel, subfamily V, member 1; TRPV2, Transient receptor potential cation channel, subfamily V, member 2; TTBS, TBS plus 0.5% Tween 20, pH 7.4; TUNEL, Terminal deoxynucleotidyl transferase dUTP nick end labelling.

Summary

Background. Cannabinoid receptor activation induces prostate carcinoma cell (PCC) apoptosis, but plant cannabinoids other than Δ^9 -tetrahydrocannabinol (THC), which lack strong activity at cannabinoid receptors, have not been investigated. Some of these compounds antagonize transient receptor potential melastatin type-8 (TRPM8) channels, the expression of which is necessary for androgen receptor (AR)-dependent PCC survival. **Experimental approach.** We tested pure cannabinoids and extracts from *Cannabis* strains enriched in certain cannabinoids (BDS), on AR-positive (LNCaP and 22RV1) and -negative (DU-145 and PC-3) cells, by evaluating: 1) cell viability with the MTT test, 2) cell-cycle arrest and apoptosis induction, by FACS scans, caspase 3/7 assays, DNA fragmentation and TUNEL, and 3) size of xenograft tumors induced by LNCaP and DU-145 cells. **Key results.** Cannabidiol (CBD) exerted a significant inhibition of cell viability. Other compounds became efficacious in cells deprived of serum for 24 hours. Several BDS were more potent than pure compounds in the presence of serum. Intra-peritoneal CBD-BDS potentiated the effects of bicalutamide and docetaxel against LNCaP and DU-145 xenograft tumors, respectively, and per se reduced LNCaP xenograft size. CBD (1-10 μ M) induced apoptosis and markers of intrinsic pathways thereof, i.e. PUMA and CHOP expression and intracellular Ca^{2+} . In LNCaP cells, the pro-apoptotic effect of CBD was only partly due to TRPM8 antagonism and was accompanied by down-regulation of AR, p53 activation and elevation of reactive oxygen species. LNCaP cells differentiated to androgen-insensitive neuroendocrine-like cells were more sensitive to CBD-induced apoptosis. **Conclusions.** These data support the clinical testing of CBD against prostate carcinoma.

Key words: prostate; cannabinoid; TRP channel; apoptosis; ROS; androgen.

Introduction

The rapid progress of the research on cannabinoids has contributed to the understanding of the biological actions of these molecules and of their medical significance, which encompass a broad spectrum of physiological and pathological mechanisms in diverse cell types [Bab I., 2011]. Cannabinoids are used for the treatment of nausea and vomiting, two common side effects accompanying chemotherapy in cancer patients [Robson, 2005; Galal *et al*, 2009]. Evidence also indicates that Δ^9 -tetrahydrocannabinol (THC) and synthetic agonists of cannabinoid CB₁ and CB₂ receptors, as well as endocannabinoids, are promising regulators of malignant cell growth. In most cases, these actions have been attributed to the ability of these compounds to activate the cannabinoid receptors or, as in the case of anandamide, also the transient receptor potential (TRP) vanilloid type-1 (TRPV1) channel [Munson *et al*, 1975; De Petrocellis *et al*, 1998; Maccarrone *et al*, 2000; Bifulco *et al*, 2001; Jacobsson *et al*, 2001; Sánchez *et al*, 2001; Casanova *et al*, 2003; Ligresti *et al*, 2003; Mimeault *et al*, 2003; Contassot *et al*, 2004; Caffarel *et al*, 2010; Guindon and Homann, 2011]. Cannabinoid receptor agonists, apart from their pro-apoptotic and anti-proliferative anticancer activities, may affect also tumor cell angiogenesis, migration, invasion, adhesion, and metastasization [Blázquez *et al*, 2003; Portella *et al*, 2003; Preet *et al*, 2008]. Non-THC cannabinoids have also been tested in cancer [Izzo *et al*, 2009; Gertsch *et al*, 2010; Russo, 2011]. Cannabidiol (CBD), for example, which is very abundant in certain strains of *Cannabis*, has very low affinity for CB₁ and CB₂ receptors, and activates TRPV1 channels [Bisogno *et al*, 2001], induces apoptosis in a triple-negative breast carcinoma cell line, and inhibits its growth and metastasis in vivo [Ligresti *et al*, 2006; Ramer *et al*, 2010; McAllister *et al*, 2011; Aviello *et al*, 2012]. Together with CBD, other non-THC cannabinoids (i.e. cannabigerol [CBG], cannabichromene [CBC], cannabidiolic acid [CBDA] and Δ^9 -tetrahydrocannabidiolic acid [THCA]) were also assessed on a wide panel of tumoral cell lines distinct in origin and typology, in comparison with extracts (known as “botanical drug substances”, [BDS]) from corresponding *Cannabis* strains enriched in these compounds [Ligresti *et al*, 2006]. Indeed, the testing of a BDS enriched in a certain cannabinoid might reveal the presence of potentially important synergistic effects between cannabinoid and non-cannabinoid cannabis components, which might be useful from a therapeutic point of view. The results obtained indicated that, of these five pure compounds and BDS tested, CBD and CBD-BDS were usually the more effective inhibitors on cancer cell growth, with little or no activity in non-cancer cells [Ligresti *et al*, 2006]. CBD inhibits also glioblastoma growth, and potentiates the action of THC on this type of tumor [Torres *et al*, 2011]. These effects seem to involve cannabinoid and TRPV1 receptors only to a small extent [Massi *et al*, 2004; Vaccani *et al*, 2005; Torres *et al*, 2011].

Prostate carcinoma is a major life-threatening disease in men and, according to the WHO, the cases of death caused by this type of cancer will have doubled within the next 30 years [Bahnson, 2007; Jemal *et al*,

2009], thus urgently calling for novel therapeutic approaches for its treatment. Endocannabinoids through CB₁ receptors, and synthetic endocannabinoid-vanilloid hybrids via stimulation of TRPV1, were shown to inhibit nerve growth factor (NGF)-induced proliferation of human prostate PC-3 cells [Melck *et al*, 2000]. However, THC can both induce apoptosis of these cells via a receptor-independent mechanism [Ruiz *et al*, 1999], and increase the production therein of the pro-proliferative factor, NGF [Velasco *et al*, 2001]. A role for CB₂ receptors in the induction of prostate carcinoma cell (PCC) apoptosis emerged recently [Sarfraz *et al*, 2005; Olea-Herrero *et al*, 2009], whereas the prototypical TRPV1 agonist, capsaicin, produces both pro-proliferative and pro-apoptotic effects on PCCs [Sánchez *et al*, 2005; Sánchez *et al*, 2006; Czifra *et al*, 2009; Ziglioli *et al*, 2009; Malagarie-Cazenave *et al*, 2009; Malagarie-Cazenave *et al*, 2011], and not necessarily via TRPV1 activation, depending on their sensitivity to androgen. To add further complexity to this scenario, other TRP channels have been suggested to play a role in PCC survival. TRP channels of melastatin-type 8 (TRPM8) are over expressed in androgen-dependent PCC lines in a manner dependent on androgen receptor (AR) activation [Horoszewicz *et al*, 1983; Tsavaler *et al*, 2001; Henshall *et al*, 2003; Zhang and Barritt, 2004; Bidaux *et al*, 2005; Bidaux *et al*, 2007]. By contrast, TRP channel of vanilloid type-2 (TRPV2) are down-regulated by AR, and their activation stimulates PCC migration [Monet *et al*, 2010]. These findings became very relevant to current investigations of the anti-tumor activity of non-THC cannabinoids, when it was found that many such compounds, and the corresponding BDS, antagonize TRPM8 channels and activate and subsequently desensitize TRPV2 and TRPV1 channels [Qin *et al*, 2008; De Petrocellis *et al*, 2008; De Petrocellis *et al*, 2011]. Furthermore, most of these compounds are also able of inhibiting endocannabinoid inactivation [De Petrocellis *et al*, 2011]. Therefore, they might act as “indirect” cannabinoid receptor agonists, similar to synthetic compounds previously found to inhibit prostate carcinoma cell growth [Nomura *et al*, 2011].

Based on this background, we tested twelve pure cannabinoids and nearly all the corresponding BDS on PCC growth in vitro and in vivo. We investigated the cellular and molecular mechanisms of the putative effects of these compounds using both AR-positive and -negative PCC lines, under different culturing conditions, in the presence or absence of currently used chemotherapeutic agents, and after differentiation into a more malignant phenotype. By employing pharmacological, molecular biology, cell biology and immunofluorescence techniques in vitro, as well as xenograft tumor and survival studies in athymic mice, we suggest that non-THC cannabinoids, and CBD in particular, like THC, but without the typical psychotropic effects of this compound, might provide the bases for the development of novel therapeutic strategies for the treatment of prostate carcinoma.

Methods

Compounds and Cannabis extracts

Drug, receptor and channel nomenclature have been used according to “Guide to receptors and channels” [Alexander *et al*, 2011]. CBC (cannabichromene); CBD (cannabidiol); CBG (cannabigerol); CBN (cannabinol); CBDA (cannabidiol acid); CBGA (cannabigerol acid); CBDV (cannabidivarin); CBGV (cannabigevarin); THC (Δ^9 -tetrahydrocannabinol); THCA (Δ^9 -tetrahydrocannabinol acid); THCV (Δ^9 -tetrahydrocannabivarin); THCVA (Δ^9 -tetrahydrocannabivarin acid); and the corresponding BDS (Botanical Drug Substance – extracts prepared from *Cannabis sativa* L. Botanical Raw Material (BRM)) were provided by GW Pharmaceuticals Ltd. (Salisbury, UK). The compounds were at least 95% pure. The amount of each principal cannabinoid in the corresponding BDS varied between 40% and 70% (% w/w of extract) depending upon the BDS tested. A description of the cannabinoid content of the BDS is provided in the Supplementary section. The percent amount of each major cannabinoid in the BDS was used to calculate the amount of the BDS necessary to obtain the equimolar amount of the corresponding pure cannabinoid in the various experiments. The chemical profile of minor cannabinoids present in each BDS was unique to each BDS, as was that of non-cannabinoid components. Thus, each BDS has a unique chemical profile (“chemical fingerprint”).

Cell cultures

Human prostate epithelial PC-3, DU-145, 22RV1 and LNCaP cells were purchased from Deutsche Sammlung von Mikroorganismen und Zellkulturen GmbH (DSMZ, Braunschweig, Berlin, Germany) and were maintained at 37°C in a humidified atmosphere containing 5% CO₂. Cells were cultivated according to the information provided in each case by the supplier company. DU-145 and LNCaP cells were cultivated in RPMI-1640 medium supplemented with 10% foetal bovine serum (FBS), 100 U/ml penicillin and 0.1mg/ml streptomycin. PC3 cells were cultivated in 45% RPMI-1640 and 45% Ham's F12 medium supplemented with 10% foetal bovine serum (FBS), 100 U/ml penicillin and 0.1mg/ml streptomycin. 22RV1 cells were cultivated in 40% RPMI-1640 and 40% DMEM medium supplemented with 20% foetal bovine serum (FBS), 100 U/ml penicillin and 0.1mg/ml streptomycin. Low cell passages (between 5 and 20) were used for the study. PC-3 and DU-145 cells are androgen-independent, i.e. they do not need androgen to grow nor is their growth affected by androgens. 22RV1 cells are androgen-independent/androgen-responsive, i.e. androgens are not required for growth but stimulate growth. LNCaP cells are androgen-dependent, i.e. they require androgens in the culture medium in order to grow [van Bokhoven *et al*, 2003].

Quantitative RT-PCR analyses

Total RNA was extracted from cell pellets in 1.0 ml of Trizol® (Invitrogen) following manufacturer's instructions, dissolved in RNA storage solution (Ambion), UV-quantified by a Bio-Photometer® (Eppendorf), and stored at -80°C until use. RNA aliquots (5 µg) were digested by RNase-free DNase I (Ambion DNA-free™ kit) in a 20 µl final volume reaction mixture to remove residual contaminating genomic DNA. After DNase digestion, concentration and purity of RNA samples were evaluated by the RNA-6000-Nano® microchip assay using a 2100 Bioanalyzer® equipped with a 2100 Expert Software® (Agilent) following the manufacturer's instructions. For all samples tested, the RNA integrity number was greater than 7 relative to a 0–10 scale. 1 µg of total RNA, as evaluated by the 2100 Bioanalyzer, was reverse-transcribed in cDNA and analyzed as previously described [Grimaldi *et al*, 2009]. Optimized primers for SYBR-green analysis and optimum annealing temperatures were designed by the Allele-Id software version 7.0 (Biosoft International) and were synthesized (HPLC-purification grade) by MWG-Biotech. In the presence of splicing variants, all the sequences were aligned and the primers were designed in the homologous regions. Primer sequences are listed in Supplementary Table 1. Relative gene expression calculation, corrected for PCR efficiency and normalized with respect to the reference gene (RNA polymerase II subunit, Acc Z27113). was performed by the IQ5 software, as previously described [Grimaldi *et al*, 2009].

Western blots

Cell pellets were homogenized in cold lysis buffer containing: 50mM Hepes pH 7.4, 1% Triton X-100, 0.25% sodium hydroxicholate, 150 mM NaCl, 2 mM EDTA, 10% glycerol, 1 mM Benzamidine, 1 mM PMSF, 1/100 stock dilutions of a protease Inibitory Cocktail (Sigma-Aldrich) and 10 µl of phosphatase inhibitors (Sigma-Aldrich). Protein extracts were quantified according to Bradford's method (Bio-Rad). Sample were diluted 1:1 by Laemmli sample buffer containing 5% β-mercaptoethanol and denaturated at 95°C for 5 min. 50µg of protein for lane were separated on a Criterion TGX-stain free pre-casted 4-20% SDS gel at 150 volt. Proteins were blotted to a PVDF membrane at 100 V for 50 min in cold Tris-glycine buffer, 20% methanol and the membrane was blocked in 1xTBS (Bio-Rad) containing 1% casein (Roche) over night at 4°C. The membrane was incubated for 1 hour at room temperatures with rabbit polyclonal antibody to TRPM8 (GeneTex) diluted to 1/1000 in blocking solution or purified mouse anti-human p53 DO-1 (BD Pharmingen) or purified mouse anti-p53 (pS46) (BD Pharmingen) both diluted 1/250. TRPM8 transfected HEK-253 cells [De Petrocellis *et al*, 2008] and HeLa cells were used as positive control for TRPM8 and p53, respectively. The membrane was washed twice with TTBS (TBS plus 0.5% Tween 20, pH 7.4) and twice with blocking solution at room temperature for 10 min. Primary antibody was detected by a goat anti-rabbit or anti-mouse horseradish peroxidase-conjugated secondary antibodies (Bio-Rad) diluted 1/2000 in blocking solution. After four times washing with TTBS and a final wash by TBS, bound secondary antibody was visualized by the chemiluminescent Immun-Star Western C kit. Chemiluminescence values were collected and processed

as described for the caspase 3/7 assay. The membranes were stripped at room temperature for 15 minutes using CHEMICON re-blot plus strong antibody stripping solution (Millipore, Schwalbach, Germany) and re-probed with rabbit polyclonal antibody against β -actin (ENZO Life Sciences) diluted 1/500 in blocking solution.

MTT assay

Cells were seeded in presence of 10% FBS in 6-well dishes with varying density depending on the cell line (from 6×10^4 to 1×10^5 cells/well), and submitted to different treatment protocols. When the treatments were conducted in presence of serum after the adhesion, cells were treated with increased concentrations of compounds for 72h (the presence of serum was maintained during the treatments). When the treatments were conducted in absence of serum, after the adhesion, cells were serum-deprived for 16h and subsequently treated with increased concentrations of compounds for 24h (the absence of serum was maintained during the treatments). When the treatments were conducted in a protein deprived serum, FBS was protein-deprived by centrifugation at $3000 \times g$ in Centriplus 30kDa centrifugal filter devices (Millipore, Milan, Italy) and cells were directly seeded in presence of the above 10% protein-deprived serum and treated in those conditions with increased concentrations of compounds for 72h. Cell viability was assessed by the MTT assay. The ability of cells to reduce MTT provided an indication of the mitochondrial integrity and activity and has been interpreted as a measure of cell viability. Absorbance at 620 nm was read on a GENius-Pro 96/384 Multifunction Microplate Reader (GENios-Pro, Tecan, Milano, Italy). All compounds were dissolved in DMSO or Ethanol. Freshly stock solutions were prepared the day of the experiment. The final percent of solvent used was less than 0.1% per well. Optical density values from vehicle-treated cells were considered as 100% of MTT reducing activity and the effects were measured as a % of the inhibition of the measures obtained with vehicle alone. When several concentrations of compounds or BDS were tested, data are reported as means \pm SD of IC_{50} values calculated from three independent experiments. Statistical differences between groups were assessed by ANOVA followed by Bonferroni test by using GraphPad Instat software.

Measurement of caspase 3/7 activity

Apoptosis was evaluated by means of the Caspase-Glo[®] 3/7 Chemiluminescent Assay Kit (Promega -USA) following the manufacturer's protocol. Human prostate carcinoma DU145, LNCaP, PC3 and RV21 cells were cultured in presence of drugs in different conditions for times indicated. After incubation, cells were trypsinized when needed, washed with PBS, and processed. The assay was performed in 96-wells white-walled plates, adding 100 μ l of Caspase-Glo[®] 3/7 reagent to each well containing 1×10^4 and 2×10^4 cells in 100 μ l of culture medium. After 1 h incubation in the dark at room temperature, luminescence was

measured by a VersaDoc MP System equipped by the Quantity One® version 4.6 software (Bio Rad). All samples were assayed at least in triplicate. Luminescence values from the blank reaction (vehicle treated cells) were subtracted from experimental values. In order to evaluate the commitment to apoptosis of PCCs, cells grown in presence of vehicle were treated for 24 h with 0.1 µg/ml S-(+)-Camptothecin (Sigma-Aldrich) plus 0.2 µg/ml Anti Fas-antibody (Roche), two compounds known to potentially induce apoptosis. Statistical analysis was performed by analysis of variance at each point using ANOVA followed by Bonferroni's test.

DNA fragmentation analyses

Analysis of DNA fragmentation was performed essentially as described in the Agilent tech-note number 5988-8028EN. Briefly, cell pellets containing about 2×10^6 cells were gently resuspended at 4°C in 100 µl of lysis solution (0.2% Triton X-100, 10 mM Tris pH 8, 10 mM EDTA) and incubated for 5 min. After centrifugation at 13000 x g the supernatants were purified by a QIAquick PCR purification kit (QIAGEN) (elution volume 30 µl). 1 µl from each samples was run in a Agilent 2100 bioanalyzer with the DNA 7500 Lab Chip kit (Agilent), following the manufacturer's instruction.

FACS scan analyses

1 ml of 70% ethanol at 4°C was added drop by drop to the cell pellets by gently mixing. After incubation for 30 min, ethanol was discarded and the cell were washed twice by 1 ml of PBS, spinning down at 400xg for 5 min. Pellets were resuspended in 250 µl of PBS containing RNase A –DNase free (100 µg/ml) and incubated at 37°C for 30 min. Propidium iodide was added at final concentration of 20 µg/ml and incubation (starting from 30 min to 2 h) was performed on the dark in ice until Flow Cytometry analysis. FACS analysis was performed to FACS-facility service of IGB-IBP of CNR-Naples, Italy by using a Becton-Dickinson FACS model CantoR. Statistical analysis was performed by the program ModFit LT version 3.0 (Verity Software House).

TUNEL assays using a bioanalyzer

The kit: "In situ cell death Detection kit, Fluorescein" (Roche) was used for these analyses After incubation with the compounds, cells were collected into 15ml tubes (Falcon, BD Biosciences) and washed twice with PBS and centrifuged at 250 rpm for 5min at R.T.. The pellet was resuspended in the fixative solution (4% paraformaldehyde) and incubated for 1 hour in agitation. After two washes with PBS, to remove all the paraformaldehyde, the cells were incubated for 2min in the permeabilization solution (0,1% TritonX-100, 0,1% sodium citrate) on ice. After two washes, the pellet obtained was resuspended in 100µl of the TUNEL Reaction Mixture (400 µl Labeling Solution plus 100 µl of the enzymatic solution) and incubated for 1 hour in humidified atmosphere in the dark. Then, cells were washed, resuspended in 250µl of ethanol 70%, treated with 20µg/ml of Propidium iodide and the suspension was incubated for 30min on ice in the dark.

The cells were then resuspended in Cell Buffer (Agilent Technologies). Fluorescence was evaluated using a Bioanalyzer equipped with 2100 Expert Software (Agilent Technologies).

TUNEL and TRPM8 immunofluorescence measurements

LNCaP and DU-145 cells attached on slides (Deckglaser, 21 × 26 mm) in six-well culture plates, both after CBD treatment or just serum deprivation, were used for TRPM8 and TUNEL double staining or TRPM8/calnexin double immunoreaction. After removal of cell culture media and three brief and delicate rinses in PBS, the cells were 20 min fixed in paraformaldehyde solution (4% in PB on agitation at +4°C) and then washed twice in PBS. For TRPM8 immunohistochemistry and TUNEL double staining the cells were incubated overnight +4°C with primary rabbit polyclonal anti-TRPM8 antibody (GeneTex, Irvine, CA, USA) diluted 1:400 in phosphate buffer solution (PBS, pH = 7.4, 0.1 M) and then incubated 4 h at +4°C with donkey anti-rabbit secondary antibody Alexa-Fluor 546 diluted 1:200 in PBS. After rinsing in PBS the same cells were processed for the TUNEL assay performed using commercial in situ cell death detection kit fluorescein (Roche diagnostic GmbH, Mannheim, Germany) in accordance with the manufacturer's instructions. Briefly, the cells were incubated in the TUNEL reaction mixture prepared immediately before use mixing the enzyme solution of terminal deoxynucleotidyl transferase enzyme (E) with the label solution of nucleotide mixture in reaction buffer. After 60 min incubation at 37°C in the dark and humidified atmosphere the cells were rinsed in PBS and embedded with antifade prior mounting with coverslip. Negative control of TUNEL reaction was performed by incubation of CBD-treated LNCaP cells with label solution without enzyme terminal transferase instead of the TUNEL reaction mixture. No signal was observed after this treatment.

In order to provide evidence for the localization of TRPM8 receptor in the endoplasmic reticulum, the TRPM8/calnexin double immunoreaction was performed in LNCaP cells after 30 min permeabilization in 0.1% Triton X-100 PB solution and overnight incubation at +4°C in a mixture of anti-rabbit TRPM8 (GeneTex, Irvine, CA, USA) and anti-goat calnexin (Santa Cruz Biotechnology, Santa Cruz, CA USA) primary antibodies, both diluted 1:400 in 0.1% Triton X-100 PB solution. Subsequently, the cells were rinsed in PBS and reacted 4 h at +4°C with a mixture of donkey anti-goat Alexa 546 and donkey anti-rabbit alexa 488, both diluted 1:200 in 0.1% Triton X-100 PB solution. DAPI nuclear counterstaining was performed before mounting the slices. Immunocytochemical TRPM8 negative control included pre-absorption of diluted anti-TRPM8 antibody with immunizing peptide or omission of either TRPM8 and Calnexin primary antisera. These experiments did not show any immunostaining. All the samples were observed at fluorescence microscope Leica DM16000B equipped with objective at differential interference contrast, appropriate filters and deconvolution system. Images were acquired by using the digital camera Leica DFC420 connected to the

microscope and the image analysis software Leica MM AF Analysis Offline for Z-stack acquisition (Leica, Germany).

Intracellular calcium and reactive oxygen species assays

Prostate cells were grown on 100-mm diameter Petri dishes as described and maintained under 5% CO₂ at 37°C. On the day of the experiment, the cells were loaded for 1 h at 25°C with the selective cytoplasmic calcium indicator Fluo-4AM (Invitrogen), 4 μM in DMSO containing 0.02% Pluronic F-127 (Invitrogen). After loading, cells were washed twice in Tyrode's buffer (145 mM NaCl, 2.5 mM KCl, 1.5 mM CaCl₂, 1.2 mM MgCl₂, 10 mM D-glucose, and 10 mM HEPES, pH 7.4), resuspended in the same buffer, and transferred to the quartz cuvette of the spectrofluorimeter ($\lambda_{\text{EX}}=488$ nm, $\lambda_{\text{EM}}=516$ nm) (Perkin-Elmer LS50B equipped with PTP-1 Fluorescence Peltier System; PerkinElmer Life and Analytical Sciences, Waltham, MA) under continuous stirring. Experiments were carried out by measuring cell fluorescence at 25 °C before and after the addition of various concentrations of the test compounds. Agonist activity was determined in comparison to the maximum increase of intracellular Ca²⁺ due to the application of 4 μM ionomycin (Alexis Biochemicals, Lausen Switzerland). EC₅₀ values were determined as the concentration of test substances required to produce half maximal increase in [Ca²⁺]_i. In some experiments, cells were loaded with Fura-2-AM (2.5 μM) in Ca²⁺-free buffer solution containing MgCl₂ in amounts equivalent to CaCl₂ and 0.1 mM EGTA. The dye was excited at 340 and 380 nm to monitor relative [Ca²⁺]_i changes by the F₃₄₀/F₃₈₀ ratio, and the emission was at 540 nm. Changes in fluorescence were monitored after a 5 min stabilization period, in a 0–300 s time interval after cell stimulation. All determinations were performed at least in triplicate. Curve fitting (sigmoidal dose–response variable slope) and parameter estimation was performed with GraphPad Prism® (GraphPad Software Inc., San Diego, CA). Statistical analysis of the data was performed at each point using ANOVA followed by Bonferroni's test.

Intracellular reactive oxygen species (ROS) generation was determined by spectrofluorometric analysis. PCCs were plated (1 x 10⁶ cells/petri) for 24 h. The day of the experiment, cells were rinsed once with Tyrode's buffer, then loaded (1 h at 37°C in darkness) with 10 μM 2',7'-dichlorofluorescein diacetate (fluorescent probe; Molecular Probes, Eugene, OR). Reactive ROS-induced fluorescence of intracellular 2',7'-dichlorofluorescein diacetate was measured with a microplate reader (PerkinElmer LS50B, $\lambda_{\text{EX}}=495$ nm; $\lambda_{\text{EM}}=521$ nm). Fluorescence detections were carried out after the incubation of 100 μM H₂O₂ and/or increasing concentrations of cannabinoids at room temperature in the darkness for different times (0–30–60–120 min). The fluorescence measured at time 0 was considered as basal ROS production and subtracted from the fluorescence at different times (Δ_1). Data are reported as mean ± S.E. of Δ_2 , i.e., fluorescence Δ_1 values at different doses subtracted of the Δ_1 values of cells incubated with vehicle. In some experiments, a

buffer containing $MgCl_2$ in amounts equivalent to $CaCl_2$ and 0.1 mM EGTA and cells preloaded for 30 min with BAPTA-AM (40 μM) were used instead.

In vivo xenograft assays of anti-tumor activity

These test were performed at PRECOS, UK, by Dr. David Kendall, whose valuable help is acknowledged. Male MF-1 nude mice aged 4-7 weeks old (supplier: Harlan, UK) were used for the study. Mice were maintained in sterile isolators within a barriered unit illuminated by fluorescent lights set to give a 12 hour light-dark cycle (on 07.00, off 19.00). The room was air-conditioned by a system designed to maintain an air temperature range of $23 \pm 2^\circ C$. Mice were housed in social groups of 5 during the procedure in plastic cages (Techniplast UK) with irradiated bedding and provided with both nesting materials and environmental enrichment. Mice were fed on sterile irradiated 2019 rodent diet (Harlan Teckland UK) and autoclaved water will be offered ad libitum. Animal welfare was checked daily. Unexpected adverse effects were noted and detailed in the final report and also reported to the Named Animal Care and Welfare Officer (NACWO) and Named Veterinary Surgeon (NVS). Animals could be terminated at any time during the study if any unexpected adverse effects are noted according to Home Office Project Licence. Each animal was allocated a unique identification number by implantation of a transponder.

There were 6 experimental groups for each cell line studied (LNCaP and DU-145 cells), with 10 mice per group; the groups consisted of the following:

Group 1	Vehicle
Group 2	1 mg/kg CBD BDS i.p. daily.
Group 3	10 mg/kg CBD BDS i.p. daily
Group 4	100 mg/kg CBD BDS i.p. daily
Group 5	either 5 mg/kg Taxotere i.v. once weekly or 25-50 mg/kg Casodex p.o. three times per week
Group 6	100 mg/kg CBD BDS i.p. daily plus either 5mg/kg Taxotere i.v. once weekly or 25-50 mg/kg Casodex p.o. three times per week

For the LNCaP xenograft studies, LNCaP cells were maintained in vitro in RPMI culture medium (Sigma, UK) containing 10% (v/v) heat inactivated foetal bovine serum (Sigma, Poole, UK), 2 mM L-glutamine (Sigma, UK) at 37°C in 5% CO_2 and humidified conditions. Cells from sub-confluent monolayers were harvested with 0.025% EDTA, washed in culture medium and re-suspended in matrigel for in vivo administration at 1-

2×10^7 cells in 200 μ l and were injected subcutaneously into the left flank of mice. The mice were anaesthetized and a 0.5 mg 5-alpha-dihydrotestosterone pellet (21-day release; Innovative Research of America, US) was implanted subcutaneously into the scruff of each mouse to facilitate the initial xenograft implant and growth. The wound was closed with Michel clips.

For the CBD-BDS DU145 cell study, the cells were maintained in vitro in RPMI culture medium (Sigma, UK) containing 10% (v/v) heat inactivated foetal bovine serum (Gibco, Paisley, UK) at 37°C in 5% CO₂ and humidified conditions. Cells from sub-confluent monolayers were harvested with 0.025% EDTA, washed in culture medium and re-suspended in matrigel for in vivo administration at 5×10^5 cells in 200 μ l and were injected subcutaneously into the left flank of mice. Tumor dimensions were recorded at Day 7 (calliper measurement of length and width and tumor cross-sectional area and volume calculated) and were recorded three times weekly and body weight measured weekly. When the tumor volume reached between 100-200 mm³ (2-3 weeks) mice were allocated to their treatment groups. Mice were evaluated daily by an experienced technician for 4-5 weeks. CBD-BDS was formulated in 1:1:18 ethanol:Cremophor:0.9% saline as follows: CBD-BDS was weighed into glass vial and dissolved in ethanol to 20x final concentration and vortexed. CBD BDS was prepared daily from ethanol stocks stored at -20°C. An equal volume of Cremophor was added and vortexed. Finally 18 times the volume of saline was added to the solution and vortexed. Compounds were prepared on a weekly basis and stored at 4°C. The final concentration of the dosing solutions was determined according to the mean weight of the mice in each group at the start of the study and weekly thereafter. Each animal remained in the study until terminated, or until necessitating removal of that mouse from the study. Animals could have been terminated at any time during the study if the tumor size became excessive or any adverse effects are noted according to the applicable UK Home Office Project Licence. At termination, the mice were anaesthetised (Hypnorm/Hynovel) and blood removed by cardiac puncture, processed for plasma and frozen at -20°C. The mice were then be terminated by decapitation. Tumors were excised, weighed, half fixed in formalin and embedded into paraffin, half frozen and stored at -20°C. For the first CBD DBS Bicalutamide LNCaP study, dosing was initiated on day 15 and study terminated day 38. For the second CBD-BDS Bicalutamide LNCaP studies, mice were terminated in a staggered manner based on tumor volume exceeding 1700 mm³, and data were presented as a survival plot.

Results

Expression of TRP channels in PCC lines under various experimental conditions

As shown by quantitative-real time PCR analyses, all four cell lines expressed at least one of the four TRP channels investigated, under all culturing conditions (Supplementary Fig. 1A and data not shown). All PCCs, except LNCaP cells, expressed TRPV1 and TRPA1 channels. TRPV2 was expressed in DU-145 and PC3 cells only. LNCaP cells and, to a smaller extent, PC3 cells, expressed only the short variant of TRPM8 channels, the mRNA of which, in the former cells, was down-regulated following serum-deprivation (see below). Addition of testosterone partly reversed TRPM8 down-regulation, in agreement with previous literature [Zhang and Barritt, 2004; Bidaux *et al*, 2005]. (see below). Unlike previously suggested [Monet *et al*, 2010], however, no up-regulation of TRPV2 channels was observed following even prolonged serum deprivation in LNCaP cells (data not shown). Although TRPM8 mRNA was reduced already by a 24 h serum-deprivation (see below), the TRPM8 protein was not, as shown by Western blot (Supplementary Figure 1C) and immunocytofluorescence analyses (see below). Finally, CB₁ and CB₂ receptors were abundantly expressed in PC3 cells, much less so in LNCaP cells, whilst DU-145 cells expressed some CB₂ mRNA and 22RV1 cells some CB₁ mRNA (Supplementary Fig. 1B).

Effect of cannabinoid receptor or TRP channel agonists and antagonists on PCC viability in MTT assays

We tested well established agonists and antagonists of TRP channel and cannabinoid receptors in LNCaP and DU-145 cells using the MTT assay (Supplementary Fig. 2). Relatively low concentrations of capsaicin, but not resiniferatoxin, evoked a small albeit significant stimulatory effect on the viability of both cell lines (Supplementary Fig. 2A). Only very high and likely non-selective doses of capsaicin, and much less so RTX, inhibited cell viability, and these effects were not antagonized by the selective TRPV1 antagonist, I-RTX (data not shown). Allylthiocyanate, a TRPA1 agonist, inhibited cell viability, but this effect was not reversed by two different TRPA1 antagonists, HC030031 and AP18 (Supplementary Fig. 2B). Finally, icilin, a synthetic TRPM8 agonist, evoked a small albeit significant stimulatory effect on the viability of LNCaP, but not DU-145, cells, whereas phenyl-4-phenyl (-)-menthylamine (OMDM233), a selective TRPM8 antagonist [Ortar *et al*, 2010], inhibited LNCaP, but not DU-145, cell viability (Supplementary Fig. 2C). The effect of this compound reached a plateau of 25-30% inhibition already at a 1 μ M concentration (which corresponds to its IC₅₀ at the rat recombinant TRPM8 [Ortar *et al*, 2010]), and higher concentrations did not cause stronger inhibition. A strong inhibitory effect of dual CB₁/CB₂ agonists (HU210, WIN55,212-2) was observed on both DU-145 and LNCaP cells, but only at concentrations (> 5 μ M) incompatible with their K_i for cannabinoid receptors (Supplementary Fig. 2D). This effect was not antagonized by SR141716 or SR144528 (0.5 μ M), two CB₁- and CB₂-selective antagonists, respectively (Supplementary Fig. 2D). Studies in other cancer cells (human colorectal carcinoma Caco-2 cells) have shown effects of synthetic and endogenous cannabinoids on viability via mechanisms not involving cannabinoid receptors [see Gustafsson *et al*, 2009 for an example]. The CB₁-selective agonist ACEA, and the CB₂-selective agonist JWH133, did not exhibit any

significant effect on the two cell lines at concentrations up to 10 μM (not shown). Finally, a selective endocannabinoid uptake inhibitor (OMDM-1) inhibited cell viability only at concentrations $> 10 \mu\text{M}$ (max inhibition 51.6%, data not shown), higher than its reported IC_{50} against anandamide cellular reuptake [Ortar *et al*, 2003]. In PC3 cells, which exhibit the highest expression levels of CB1 and CB2 receptors (see above), HU210 and WIN55,212-2 only inhibited cell viability at concentrations $\geq 5 \mu\text{M}$ (data not shown).

Effect of cannabinoids and BDS on PCC viability in MTT assays

For these experiments all PCC lines were used. In particular, the complete panel of cannabinoids and relative BDS were screened in DU-145 and LNCaP in the presence and/or absence of serum, whereas only the pure compounds were screened in 22RV1 and PC-3 cells under these two conditions. As shown in Tables 1 and 2, of all non-THC cannabinoids tested in DU-145 and LNCaP cells, CBD was the most efficacious inhibitor of cell viability, followed by CBC, in presence of serum. The corresponding BDS were usually as efficacious as the pure compounds, and in many cases their effects were stronger in the presence of serum. However, a “cannabinoid-free” BDS, obtained by eliminating CBG from CBG-BDS [De Petrocellis *et al*, 2011], and tested in amounts corresponding to those present in 10 μM of CBG-BDS, was nearly inactive in both DU-145 and LNCaP cells (15 ± 5 and 26 ± 18 % inhibition, respectively, means \pm SE N=3). Importantly, and in full agreement with previous observations in glioma cells (Jacobsson *et al*, 2000), in both cell lines, pure cannabinoids and BDS became potent and efficacious at inhibiting the viability of cells previously kept for 15 hours without serum and with an additional 24 h incubation without serum. Similar results were obtained in PC3 and 22RV1 cells (Supplementary Tables 2 and 3).

As these data suggest that the presence of serum during the MTT assay might counteract the inhibitory effect of the compounds on PCC viability, we next examined in detail whether the reintroduction of BSA in serum-deprived media would reduce the inhibitory effects of CBD, CBG and CBC (Fig. 1A), or if the use of protein-deprived sera (see Methods) could restore the high potency exhibited by these compounds in conditions of serum deprivation (Fig. 1B). Only in the absence of high molecular weight proteins in the serum, the compounds exhibited good efficacy and potency at inhibiting cell viability in both cell lines. By contrast, the addition of testosterone or estradiol in a serum-deprived medium, did not significantly modify the effect of CBD (Fig. 1C).

We finally tested if various antagonists of cannabinoid receptors (SR141716 or SR144528, 0.5 μM), TRPV1 (I-RTX, 1 μM) and TRPA1 (HC030031 and AP18, 30 μM) channels, or an agonist of TRPM8 channels (icilin, 2 μM), influenced the inhibitory effects of CBD in the MTT assays under serum-deprivation conditions, and found no significant effect with any of these compounds (data not shown).

Interactions between the effect of CBD and bicalutamide or docetaxel on PCC viability in MTT assays

Standard chemotherapeutics for the treatment of prostate cancer (i.e. bicalutamide and docetaxel [DCX]) were tested on either LNCaP or DU-145 cells, cultured in the presence of serum, w/wo varying concentrations of CBD. DCX did not strongly affect *per se* the proliferation of LNCaP cells ($IC_{50} > 25 \mu\text{M}$). However, when it was tested in combination with pure CBD, an improvement of its effect was observed, even though this appeared to be due to additive effects (Supplementary Fig. 3A). DCX was more effective at inhibiting DU-145 cell growth, and CBD (only at the lowest concentration tested) potentiated the effect of this compound (Supplementary Fig. 3C). Finally, CBD significantly enhanced the efficacy of bicalutamide (10 μM) in LNCaP cells, although only at the highest dose tested (Supplementary Fig. 3B).

Effect of a CBD-enriched *Cannabis* extract on xenograft tumor growth in vivo

We carried out studies *in vivo* on the effects of DCX (taxotere), bicalutamide (casodex) and CBD-BDS on xenograft tumors obtained in athymic mice with LNCaP and DU-145 cells. CBD-BDS dose-dependently inhibited the growth of xenografts from LNCaP, but not DU-145, cells. At the highest dose tested (100 mg/kg, *i.p.*), the extract exerted on LNCaP xenografts an effect quantitatively similar to that of DCX (5 mg/kg, *i.v.*), although it reduced the tumor growth inhibitory effect of this agent (Fig. 2A), whereas it significantly potentiated it in DU-145 cell xenografts (Fig. 2B). In a second experiment with xenograft tumors from LNCaP cells, two doses (25 and 50 mg/kg, *p.o.*) of bicalutamide alone or CBD-BDS alone (100 mg/kg, *i.p.*) produced little effect on tumor weight and volume at the end of the treatment, possibly because this experiment was interrupted after only 35 days. However, co-administration of bicalutamide at 25 mg/kg and CBD-BDS significantly inhibited xenograft growth (Fig. 2C). When a Kaplan-Meier plot for survival analysis was carried out in a third experiment, lasting until 47 days of treatment, CBD-BDS plus bicalutamide significantly prolonged survival as compared to bicalutamide or CBD-BDS alone (Fig. 2D).

Effect of cannabinoids on PCC caspase 3/7 activity

When the cannabinoids or corresponding BDS were tested in LNCaP cells in the presence of serum for 24 hours, very little effect was observed on caspase 3/7 activity, and only with CBD (10 μM) and CBC (10 μM) (Fig. 3A). In DU-145 cells, only THCV, THCVA and CBGV produced a little effect (Fig. 3B). By contrast, the positive control, consisting of anti-Fas antibody plus camptothecin for 24 h, produced a strong effect in both cell lines (Fig. 3A,B). In LNCaP cells, the TRPM8 antagonist, OMDM233 (1 μM), exerted an effect similar to that of CBD, and the TRPM8 agonist icilin, at a dose producing no effect *per se* (0.05 μM), antagonized the effect of CBD (Fig. 3A). Several BDS produced stronger effects on caspase 3/7 activity in both LNCaP and DU-145 cells (Supplementary Fig. 4A,B).

When LNCaP cells were cultured under varying conditions of serum-deprivation (SDP), the effect of CBD on caspase 3/7 activity was dramatically stronger, whereas that of OMDM233 decreased (Fig. 3C). Also CBC and CBG were found to release caspase 3/7 under these conditions, although the latter compound only at a 20 μ M concentration (Fig. 3D). The extent of the effect of 10 μ M CBD varied with the time of incubation or the duration of serum-deprivation prior to incubation with the compound (Supplementary Fig. 5). As described above for the MTT assay, only in the absence of proteins in the serum CBD exhibited high efficacy at stimulating caspase 3/7 activity in LNCaP cells, whereas the presence or absence of testosterone (as in normal serum or charcoal-stripped serum, respectively) did not influence its effect (Fig. 3E). Finally, under conditions of serum-deprivation, the effect of CBD was still significantly attenuated by icilin (Fig. 3C), but not by TRPV1, CB₁ and CB₂ antagonists (I-RTX [0.2 μ M], SR141716 [0.5 μ M] or SR144528 [0.5 μ M], respectively) (Supplementary Fig. 6).

CBD (10 μ M) was also efficacious at elevating caspase 3/7 activity in DU-145 cells under varying conditions of SDP (Fig. 3F), but CBC and CBG (20 μ M) were much less active, or inactive, in these cells also under these conditions (Supplementary Fig. 7). Agonists of TRPV1, TRPV2 and TRPA1, which are highly expressed in these cells (see above), i.e. capsaicin (1 μ M), THCv (20 μ M [De Petrocellis *et al*, 2011]), and allylthiocyanate (100 μ M), respectively), were either inactive, or, when active (as in the case of allylthiocyanate), the effect was not antagonized by the respective antagonist (AP18, 30 μ M) (data not shown).

In serum-deprived 22RV1 cells (Fig. 3G) and PC3 cells (Fig. 3H), both CBD (10 μ M) and CBC (20 μ M), but much less so CBG (20 μ M), caused strong activation of caspase 3/7 (Fig. 3G,H). In the former cells, the effect of CBD was not significantly altered by the presence of testosterone (data not shown).

Effect of CBD on apoptosis as assessed by TUNEL positivity

When cells incubated with vehicle or CBD (10 μ M) under SDP leading to optimal release of caspase 3/7 were analyzed with a bioanalyser, significant TUNEL positivity was found in all PCC lines (Supplementary Fig. 8A-D, Supplementary Table 4). This was confirmed by immunofluorescence in LNCaP and DU-145 cells treated with CBD (10 μ M). Importantly, in LNCaP cells, TUNEL positivity was observed in both TRPM8-expressing and non-expressing single cells, whereas TRPM8-expressing cells were not always TUNEL positive (Supplementary Fig. 9). Interestingly, TRPM8 immunoreactivity was not significantly decreased after serum-deprivation, in agreement with the results of the western blot in Supplementary Fig. 1C, and to be localized almost uniquely in the endoplasmic reticulum [ER], since it co-stained with the ER marker calnexin (Supplementary Fig. 9), in agreement with previous studies [Bidaux *et al*, 2005; Valero *et al*, 2011].

Effect of CBD on PCC apoptosis and cell cycle

We carried out an analysis of the DNA fragmentation pattern induced by CBD (10 μ M), under conditions that optimally stimulate caspase 3/7 activity (see above). A typical apoptotic DNA fragmentation pattern was found in LNCaP cells (Supplementary Fig. 10). Furthermore, using FACS scan analyses, we could further establish that CBD, apart from inducing apoptosis in these cells (Supplementary Fig. 8E), also causes apoptosis and inhibits the G1-S transition of the cell cycle in DU-145 cells (Supplementary Fig. 8F). These results are summarized in Supplementary Tables 5 and 6. CBD also strongly elevated the expression of the cell-cycle inhibitors p27^{kip}, only in AR-expressing PCCs (Supplementary Fig. 8G), and p21, in all PCCs (4.5x, 5x, 6x and 15x in LNCaP, 22RV1, DU-145 and PC-3 cells, respectively, data not shown).

Effect of CBD on PUMA, CHOP, AR, TRPM8 and p53 expression

CBD (10 μ M), incubated with serum-deprived cells under conditions leading to optimal caspase 3/7 activation, up-regulated the transcriptional expression levels of the p53-upregulated modulator of apoptosis (PUMA), a major player in intrinsic pathways of apoptosis, in all four cell lines under investigation (Fig. 4A). CBD also elevated p53 protein expression in AR-expressing cells (Fig. 4B) and CCAAT/enhancer binding protein (CHOP) mRNA expression in all cells (Fig. 4C). In LNCaP cells, Ser46-phosphorylation on p53 was also increased on top of the effect on protein expression (Fig. 4B). Finally, CBD (10 μ M) downregulated AR mRNA in LNCaP and, to a smaller extent, 22RV1 cells (Fig. 4D,E), and reduced basal and testosterone-induced TRPM8 mRNA levels in LNCaP cells (Fig.4F).

Effect of cannabinoids on intracellular calcium and reactive oxygen species (ROS) assays

We studied whether CBD was able to induce intracellular Ca²⁺ mobilization and production of ROS in all four PCCs. Our results indicate that: 1) CBD dose-dependently elevates intracellular Ca²⁺ in all four PCC lines in a manner often potentiated by SDP and independent of the presence of extracellular Ca²⁺ (Fig. 5 and Supplementary Table 7), and at concentrations similar to those necessary to induce apoptosis; and 2) CBD activates ROS production only in LNCaP cells, in a manner dependent on SDP (Fig. 5) and inhibited by intracellular Ca²⁺ chelation by BAPTA (data not shown). Also CBC and CBG produced elevation of intracellular Ca²⁺ in all four PCC lines (Supplementary Table 7).

Effect of CBD on neuroendocrine-like differentiated LNCaP cells

Serum and androgen deprivation, as well as the presence of agents that potentiate protein kinase A-mediated signaling, i.e. IBMX+db-cAMP, causes a progressive phenotypic change in LNCaP (but not 22RV1, PC3 and DU145) cells, which start producing neuron-specific enolase (NSE) and making neurite-like structures [Bang *et al*, 1994; Cox *et al*, 1999; Marchiani *et al*, 2010]. We confirmed that, similar to prolonged (72 h) SDP, 36 h incubation of these cells with IBMX+db-cAMP in no serum is sufficient to induce

neuroendocrine-like phenotype (Supplementary Fig. 11) and over-expression of NSE (Fig. 6B). CBD (10 μ M) activated caspase 3/7 in serum-deprived, IBMX+dbcAMP-treated LNCaP cells much more efficaciously than in vehicle-treated cells (Fig. 6A). The effect was not significantly antagonized by icilin, nor mimicked by the TRPM8 antagonist, OMDM233 (Fig. 6A), and was accompanied by down-regulation of NSE mRNA (Fig. 6B), and up-regulation of PUMA and p27^{kip} mRNA (Fig. 6C,D). CBD plus IBMX+db-cAMP also caused stronger down-regulation of AR and TRPM8 than those induced by serum deprivation with or without IBMX+db-cAMP alone (Fig. 6E,F; Fig. 4).

Involvement of oestrogen receptors in CBD pro-apoptotic activity

The transcriptional expression levels of oestrogen receptors, ER α and ER β in the prostate cell lines have been extensively described in literature [Cheung *et al*, 2005; Hartel *et al*, 2004]. In particular, our data confirm in LNCaP prostate cancer cells the absence of ER α and the presence of very low (although detectable) expression levels of ER β (Supplementary Table 8). In this cell line, 17 β -estradiol did not interfere with the pro-apoptotic activity of CBD as evaluated by the caspase 3/7 assay under SDP conditions (Supplementary Fig. 12A). These data suggest that ER α and ER β are not involved in pro-apoptotic activity of CBD in LNCaP cells. A high expression of G protein-coupled estrogen receptor 1 (GPER) was observed in all prostate cancer cell lines analysed, despite differences in the relative normalized expression (Supplementary Fig. 12B). Recently, G15, a high affinity antagonist of GPER has been identified and characterized [Dennis *et al*, 2009]. We report that G15, at 1 μ M, significantly, although not completely, attenuated the pro-apoptotic effect of CBD under SDP conditions (Supplementary Fig. 12C). Furthermore, G15 dose-dependently inhibited CBD internal stores calcium release (Supplementary Fig. 12D).

Discussion

Non-THC cannabinoids inhibit PCC growth in vitro and in vivo

Starting from the recently described inhibitory activity of cannabinoids at TRPM8 [De Petrocellis *et al*, 2008; De Petrocellis *et al*, 2011;] and the proposed role of this channel in determining PCC survival [Horoszewicz *et al*, 1983; Tsavaler *et al*, 2001; Henshall *et al*, 2003; Zhang and Barritt 2004; Bidaux *et al*, 2005; Bidaux *et al*, 2007], we have carried out several experiments aimed at investigating the anti-cancer potential of non-THC cannabinoids and corresponding BDS in both AR-expressing and non-AR-expressing PCCs. Initially, we used the MTT assay of cell viability. The results obtained can be summarized as follows: 1) in full agreement with previous observations in glioma cells (Jacobsson *et al*, 2000), both cannabinoids and BDS reduce PCC viability with higher potency and efficacy in the absence of serum proteins, and regardless of the presence

of hormones in the medium and of the androgen dependency of the PCC line under study. With serum deprivation, CBD was the most efficacious compound in three out of the four cell lines investigated; 2) among all the other possible known cannabinoid targets investigated, only TRPM8, when present (as in LNCaP cells), seems to mediate, and only in part, the effect of CBD; and 3) under certain dosing conditions, CBD produces synergistic effects with DXT and/or bicalutamide in DU-145 and/or LNCaP cells.

Based on this first set of results, we decided to test CBD-BDS, administered i.p., against the growth of xenograft tumors generated in athymic mice from LNCaP and DU-145 cells. Since CBD-BDS was more efficacious in vitro than CBD in the presence of serum proteins, we administered systemically this preparation. CBD-BDS reduced tumor size *per se* in xenografts generated from LNCaP cells. In these tumors, CBD also significantly elevated the anti-cancer effect of bicalutamide, thereby significantly extending the survival time of the animals, but not those of docetaxel. Instead, CBD-BDS was inactive *per se* against the growth of DU-145 xenografts in vivo, although in this case it potentiated the effect of docetaxel. These findings suggest that *Cannabis* extracts enriched in CBD might provide the basis for new therapies against prostate carcinoma, either as standalones or in addition to currently used drugs for this type of tumor.

Cellular mechanism of action of non-THC cannabinoids

We next investigated the cellular mechanisms underlying the above effects of cannabinoids on PCCs. Since different non-THC cannabinoids might produce different effects on cell cycle and apoptosis, leading to reduced viability in the MTT assay via different mechanisms, we focused only on those compounds that were both more efficacious in this assay and usually more abundant in *Cannabis*, i.e. CBD, CBG and CBC. The results obtained can be summarized as follows: 1) the three compounds, and CBD in particular, induce caspase 3/7 activation in all four PCC lines investigated, provided that treatments are carried out under conditions of serum deprivation. The effect is insensitive to the addition of testosterone in the serum-free medium. In the presence of serum, the BDS are more efficacious than the corresponding cannabinoids; 2) CBD also inhibits the G1-S transition in DU-145 cells in FACS scan experiments, stimulates the expression of p27^{kip} in AR-expressing cells, and up-regulates the expression of p21 in all cells. CBD did not inhibit the cell cycle in FACS scan experiments carried out with LNCaP cells, possibly because these cells, unlike DU-145 cells, undergo a strong reduction of the G1-S phase transition during serum deprivation *per se*. The strong up-regulation of the expression of p27^{kip} in these cells, as well as in 22RV1 cells, but not in DU-145 and PC3 cells, is in agreement with previous data showing that this inhibitor of the cell cycle is more expressed in AR-expressing PCC lines, and less important as a cell cycle regulator in non-AR-expressing cells [Galardi *et al*, 2007].

A comparison between the results of the MTT and the caspase 3/7 activity assays allow us to make some preliminary considerations on the cellular mechanism of action of cannabinoids, and CBD in particular.

First, the anti-tumor effects of cannabinoids observed in the MTT assay in all PCCs appear to be largely due to stimulation of apoptosis. Accordingly, in both this assay and the caspase 3/7 assay, which is more amenable to the screening of pro-apoptotic effects than the DNA fragmentation or FACS scan analyses, we observed that the effects of cannabinoids were highest in the absence of serum, and the BDS were more efficacious than the corresponding pure compounds only in the presence of serum. Several possible explanations may exist for these observations. First, serum deprivation causes elimination of exogenous hormones, such as testosterone, from the medium. This, in turn, at least for the two AR-expressing cell lines employed here, might result in impaired survival mechanisms and/or inhibition of the cell-cycle (as indeed observed for LNCaP cells), and in higher vulnerability of cells to pro-apoptotic effects of compounds. However, we found that when LNCaP and 22RV1 cells were serum-deprived but kept in the presence of testosterone, the efficacy of CBD at inducing caspase 3/7 activity was not reduced, nor was its effect in the MTT assay diminished. Moreover, CBD was less, and not more, efficacious when tested in LNCaP cells kept in charcoal stripped serum, thus indicating that it is the presence of serum proteins, rather than hormones, that renders the compound less efficacious. Accordingly, addition of BSA to the serum-deprived culture medium of LNCaP cells rendered CBD inactive in both the MTT and caspase 3/7 assays. Given the high lipophilicity of cannabinoids, these observations may suggest that intracellular targets mediate their pro-apoptotic effects, and that high-MW serum proteins, such as BSA, by binding to cannabinoids, prevent them from entering the cells and interacting with these targets. Indeed, past and recent evidence has demonstrated that cannabinoids avidly bind to BSA [Papa et al., 1990; Fanali et al., 2011]. This possibility would explain why: 1) also non-androgen dependent cells were more sensitive to cannabinoids in the absence of serum; and 2) other lipophilic, non-cannabinoid *Cannabis* constituents in BDS, possibly by competing for the binding with serum proteins, increase the efficacy of cannabinoids in the presence of serum. The possibility, however, that serum deprivation, by arresting *per se* the cell cycle, as shown for LNCaP cells, predisposes cells to apoptosis independently from the absence of hormones, cannot be excluded.

Molecular mechanisms of the pro-apoptotic action of CBD

Also based on the BSA effects described above, we suggest that the pro-apoptotic effect of CBD in LNCaP cells is exerted via stimulation of intrinsic pathways of apoptosis. This was confirmed primarily by the strong elevation of PUMA mRNA levels caused by CBD. This effect, in turn, likely follows the up-regulation of the marker of ER stress, CHOP, and the activation of p53, the two stimuli for PUMA expression. CBD also induced intracellular Ca^{2+} mobilization, another marker of ER stress, and subsequent production of ROS, which, in these cells, might also contribute to apoptosis [Yu and Zhang, 2008]. Instead, in 22RV1 cells, we observed elevation of PUMA and CHOP mRNA levels and intracellular Ca^{2+} mobilization, but no ROS

elevation, nor p53 phosphorylation. Importantly, previous studies showed that stimulation of intracellular Ca^{2+} mobilization, with or without production of ROS, is stronger in serum-deprived PCCs [Gutierrez *et al*, 1999], and that CBD induces apoptosis in human breast cancer cells through intracellular Ca^{2+} and ROS elevation [Ligresti *et al*, 2006; Shrivastava *et al*, 2011], and in hepatic stellate cells via CHOP upregulation [Lim *et al*, 2011].

In both AR-expressing PCC lines used here, the effect of CBD was accompanied by down-regulation of AR mRNA, which might suggest that apoptosis was due, in part, to counteraction of the pro-survival effect of endogenously produced testosterone [Dillard *et al*, 2008; Chun *et al*, 2009]. The observed up-regulation of p53 protein expression in these cells might be either the effect or the cause of AR-down-regulation [Rokhlin *et al*, 2005; Kruse and Gu, 2009; Schiewer *et al*, 2011]. The latter, in turn, is the most likely cause of TRPM8 mRNA level reduction by CBD, since TRPM8 is under tonic stimulation by AR in AR-expressing PCCs [Zhang and Barritt, 2004; Bidaux *et al*, 2005; Bidaux *et al*, 2007; present data]. TRPM8 down-regulation, as well as direct antagonism of TRPM8 [De Petrocellis *et al*, 2008; De Petrocellis *et al*, 2011], are further mechanisms through which, in LNCaP cells (but not in 22RV1 cells, found here not to express this channel), CBD might have exerted its pro-apoptotic effects [Zhang and Barritt, 2004], which, accordingly, were attenuated by a *per se* inactive dose of a TRPM8 agonist [Ortar *et al*, 2010]. However, even in LNCaP cells other receptors must contribute to CBD pro-apoptotic effects since: 1) TRPM8 antagonism was not sufficient alone to produce a strong pro-apoptotic effect; 2) CBC, which is inactive as a TRPM8 antagonist [De Petrocellis *et al*, 2008; De Petrocellis *et al*, 2011], still activated caspase 3/7, whereas CBG, which is as potent as CBD at antagonizing TRPM8 [De Petrocellis *et al*, 2008; De Petrocellis *et al*, 2011], was much less potent in this assay. We provided here evidence that cannabinoid CB1 and CB2 receptors and TRPV1, TRPV2 and TRPA1 channels, which are variedly expressed in the two AR-expressing cell lines employed here, do not participate in the pro-apoptotic effect of CBD. Interestingly, also the effects of CBD on intracellular Ca^{2+} and ROS elevation described above are unlikely to require TRP channels and AR, since they were described in cells that do not necessarily express these proteins [Ligresti *et al*, 2006; Drysdale *et al*, 2006].

Also in non-AR-expressing cells, the pro-apoptotic effect of CBD was accompanied by up-regulation of PUMA and CHOP expression and elevation of intracellular Ca^{2+} . PC-3 cells did not express p53, in agreement previous data [van Bokhoven *et al*, 2003]. These data suggest that in these cells CBD might still act in part via ER stress and PUMA, with no involvement of AR, p53 and TRPM8.

Role of adenosine and oestrogens in CBD pro-apoptotic effects

It should not be forgotten that the pharmacological profile of cannabidiol is complex and other mechanisms might be involved. Increase in adenosine signalling is thought to be one of the mechanisms by which CBD decreases inflammation [Izzo *et al*, 2009]. In androgen-dependent and -independent human prostate

cancer cells (DU-145, PC3, and LNCaP) adenosine was recently shown to inhibit cell proliferation by arresting cell cycle progression and inducing cell apoptosis [Aghaei *et al*, 2012]. However, adenosine was shown to act via p53, whereas the effects of CBD reported here seem to involve this pathway only to a minor extent, and only in LNCaP cells. There is evidence of a role also for oestrogens in the survival of prostate cells, and as it has been suggested that cannabinoids may influence oestrogen metabolism [Lee *et al.*, 2005], we analyzed the role of oestrogen receptors in the pro-apoptotic effects of CBD. Our data demonstrate high expression of the G-protein-coupled estrogen receptor, GPER, rather than ER α and ER β , in the PCC lines used here. GPER, also known as GPR30, is an intracellular transmembrane G protein-coupled estrogen receptor, which resides in the endoplasmic reticulum, where it activates multiple intracellular signalling pathways [Revankar *et al*, 2005]. 17 β -estradiol binds to GPER, resulting in intracellular calcium mobilization and synthesis of phosphatidylinositol 3,4,5-trisphosphate in the nucleus. It has been reported that activation of GPER inhibits growth of prostate cancer cells via upregulation of p21, and induction of G2 cell-cycle arrest [Chan *et al*, 2010, Ren *et al*, 2012]. In order to evaluate the involvement of GPER in CBD pro-apoptotic effects, a specific antagonist for this receptor, G15, which shows little affinity for ER α or ER β at concentrations up to 10 μ M, was used. Our data show that G15 was able to attenuate both CBD activation of caspase 3/7 and CBD-induced calcium release from intracellular stores in LNCaP cells, suggesting that GPER, rather than oestrogen metabolic enzymes [Lee *et al.*, 2005] or ER α or ER β [see also Ruh *et al.*, 1997], may be one of the intracellular targets through which CBD stimulates the ER branch of the intrinsic pro-apoptotic pathway.

Effect of CBD on differentiated, non-AR-expressing, neuroendocrine-like LNCaP cells

Prolonged androgen deprivation and/or activation of the protein kinase A cascade causes in some AR-expressing cells a neuroendocrine differentiation, consisting in the appearance of dendrite-like structures and NSE in culture, and higher metastatic potential *in vivo*. This process was suggested to underlie in part the phenomenon by which chronic chemical castration, although efficacious at combating prostate carcinoma at its onset, results in the late formation of AR antagonist-unresponsive and highly metastatic forms of the tumor [Bang *et al*, 1994; Cox *et al*, 1999; Marchiani *et al*, 2010]. Of the four PCC lines investigated here, only LNCaP cells were previously shown to undergo this process [Marchiani *et al*, 2010]. We found that neuroendocrine-like LNCaP cells become more sensitive to CBD in terms of caspase 3/7 activation and PUMA overexpression, despite the fact that they exhibit strongly reduced levels of AR and TRPM8 mRNA. The pro-apoptotic effect of CBD was no longer significantly attenuated by a TRPM8 agonist. CBD also appeared to reverse the neuroendocrine differentiation process of these cells, as it reduced NSE expression, whilst causing further AR reduction. Thus, although antagonism of TRPM8 might underlie in part the pro-apoptotic action of CBD in non-differentiated LNCaP cells, this cannabinoid still induces the

apoptosis of these cells when they become differentiated, possibly through other non-TRPM8 mechanisms of action discussed above.

Conclusions

The *in vitro* data presented here allow us to suggest that non-THC cannabinoids, and CBD in particular, retard proliferation and cause apoptosis of prostate carcinoma growth via a combination of cannabinoid receptor-independent cellular and molecular mechanisms. Our data, however, do not argue against the previously suggested role of CB₁ and CB₂ receptors in prostate carcinoma fate [Sarfraz et al., 2005; Olea-Herrero *et al*, 2009], although they do exclude the participation of these receptors in the effects of non-THC cannabinoids. Indeed, the effects reported here, together with previously reported cannabinoid receptor-mediated effects of THC on PCCs, might provide momentum to clinical studies on cannabinoids and *Cannabis* extracts as a therapy for human prostate carcinoma, either in addition to currently used treatments, or as standalones, as suggested also by our present *in vivo* data. Our additional observation that differentiation of an “androgen-dependent” cell into a more malignant and “androgen-unresponsive” phenotype increases its sensitivity to the pro-apoptotic effect of CBD might provide a new strategy to deal with the frequent loss of efficacy of AR antagonists against prostate carcinoma growth after only few years of treatment.

Acknowledgements

The authors are grateful to Drs. Stefania Petrosino and Roberta Imperatore for their valuable help with some of the experiments described here, and to GW Pharma, UK, for partly funding this study.

Conflict of interests

CGS is an employee of GW Pharma. VD is the recipient of a research grant from GW Pharma and a consultant for GW Pharma.

References

- Aghaei M, Karami-Tehrani F, Panjehpour M, Salami S, Fallahian F (2012). Adenosine induces cell-cycle arrest and apoptosis in androgen-dependent and -independent prostate cancer cell lines, LNCap-FGC-10, DU-145, and PC3. *Prostate* 72: 361-375.
- Alexander SP, Mathie A, Peters JA (2011). Guide to Receptors and Channels (GRAC), 5th edition. *Br J Pharmacol* 164: S1-324.
- Aviello G, Romano B, Borrelli F, Capasso R, Gallo L, Piscitelli F *et al* (2012). Chemopreventive effect of the non-psychoactive phytocannabinoid cannabidiol on experimental colon cancer. *J Mol Med (Berl)* (in press)
- Bab I (2011). Themed issue on cannabinoids in biology and medicine. *Br J Pharmacol* 163: 1327–1328.
- Bahnson R (2007). Androgen deprivation therapy for prostate cancer. *J Urol* 178: 1148.
- Bang YJ, Pirnia F, Fang WG, Kang WK, Sartor O, Whitesell L *et al* (1994). Terminal neuroendocrine differentiation of human prostate carcinoma cells in response to increased intracellular cyclic AMP. *Proc Natl Acad Sci U S A* 91: 5330-5334.
- Bidaux G, Flourakis M, Thebault S, Zholos A, Beck B, Gkika D *et al* (2007). Prostate cell differentiation status determines transient receptor potential melastatin member 8 channel subcellular localization and function. *J Clin Invest* 117: 1647-1657.
- Bidaux G, Roudbaraki M, Merle C, Crepin A, Delcourt P, Slomianny C *et al* (2005). Evidence for specific TRPM8 expression in human prostate secretory epithelial cells: functional androgen receptor requirement. *Endocr Relat Cancer* 12: 367-382.
- Bifulco M, Laezza C, Portella G, Vitale M, Orlando P, De Petrocellis L *et al* (2001). Control by the endogenous cannabinoid system of ras oncogene-dependent tumor growth. *FASEB J* 15: 2745-2747.
- Bisogno T, Hanus L, De Petrocellis L, Tchilibon S, Ponde DE, Brandi I *et al* (2001). Molecular targets for cannabidiol and its synthetic analogues: effect on vanilloid VR1 receptors and on the cellular uptake and enzymatic hydrolysis of anandamide. *Br J Pharmacol* 134: 845-852.
- Blazquez C, Casanova ML, Planas A, Gomez Del Pulgar T, Villanueva C, Fernandez-Acenero MJ *et al* (2003). Inhibition of tumor angiogenesis by cannabinoids. *FASEB J* 17: 529-531.
- Caffarel MM, Andradas C, Mira E, Perez-Gomez E, Cerutti C, Moreno-Bueno G *et al* (2010). Cannabinoids reduce ErbB2-driven breast cancer progression through Akt inhibition. *Mol Cancer* 9: 196.
- Casanova ML, Blazquez C, Martinez-Palacio J, Villanueva C, Fernandez-Acenero MJ, Huffman JW *et al* (2003). Inhibition of skin tumor growth and angiogenesis in vivo by activation of cannabinoid receptors. *J Clin Invest* 111: 43-50.
- Chan QK, Lam HM, Ng CF, Lee AY, Chan ES, Ng HK *et al* (2010). Activation of GPR30 inhibits the growth of prostate cancer cells through sustained activation of Erk1/2, c-jun/c-fos-dependent upregulation of p21, and induction of G(2) cell-cycle arrest. *Cell Death Differ* 17: 1511-1523.
- Cheung CP, Yu S, Wong KB, Chan LW, Lai FM, Wang X *et al* (2005). Expression and functional study of estrogen receptor-related receptors in human prostatic cells and tissues. *J Clin Endocrinol Metab* 90: 1830-1844.

Chun JY, Nadiminty N, Dutt S, Lou W, Yang JC, Kung HJ *et al* (2009). Interleukin-6 regulates androgen synthesis in prostate cancer cells. *Clin Cancer Res* 15: 4815-4822.

Contassot E, Tenan M, Schnuriger V, Pelte MF, Dietrich PY (2004). Arachidonyl ethanolamide induces apoptosis of uterine cervix cancer cells via aberrantly expressed vanilloid receptor-1. *Gynecol Oncol* 93:182-188.

Cox ME, Deebble PD, Lakhani S, Parsons SJ (1999). Acquisition of neuroendocrine characteristics by prostate tumor cells is reversible: implications for prostate cancer progression. *Cancer Res* 59: 3821-3830.

Czifra G, Varga A, Nyeste K, Marincsak R, Toth BI, Kovacs I *et al* (2009). Increased expressions of cannabinoid receptor-1 and transient receptor potential vanilloid-1 in human prostate carcinoma. *J Cancer Res Clin Oncol* 135: 507-514.

Dennis MK, Burai R, Ramesh C, Petrie WK, Alcon SN, Nayak TK *et al* (2009). In vivo effects of a GPR30 antagonist. *Nat Chem Biol* 5: 421-427.

De Petrocellis L, Ligresti A, Schiano Moriello A, Allarà M, Bisogno T, Petrosino S *et al* (2011). Effects of cannabinoids and cannabinoid-enriched Cannabis extracts on TRP channels and endocannabinoid metabolic enzymes. *Br J Pharmacol* 163: 1479-1494.

De Petrocellis L, Melck D, Palmisano A, Bisogno T, Laezza C, Bifulco M *et al* (1998). The endogenous cannabinoid anandamide inhibits human breast cancer cell proliferation. *Proc Natl Acad Sci U S A* 95: 8375-8380.

De Petrocellis L, Vellani V, Schiano-Moriello A, Marini P, Magherini PC, Orlando P *et al* (2008). Plant derived cannabinoids modulate the activity of transient receptor potential channels of ankyrin type-1 and melastatin type-8. *J Pharmacol Exp Ther* 325: 1007-1015.

Dillard PR, Lin MF, Khan SA (2008). Androgen-independent prostate cancer cells acquire the complete steroidogenic potential of synthesizing testosterone from cholesterol. *Mol Cell Endocrinol* 295: 115-120.

Drysdale AJ, Ryan D, Pertwee RG, Platt B (2006). Cannabidiol-induced intracellular Ca₂₊ elevations in hippocampal cells. *Neuropharmacology* 50: 621-631.

Fanali G, Cao Y, Ascenzi P, Trezza V, Rubino T, Parolaro D *et al* (2011) Binding of Δ^9 -tetrahydrocannabinol and diazepam to human serum albumin. *IUBMB Life* 63: 446-451.

Galal AM, Slade D, Gul W, El-Alfy AT, Ferreira D, Elsohly MA (2009). Naturally occurring and related synthetic cannabinoids and their potential therapeutic applications. *Recent Pat CNS Drug Discov* 4: 112-136.

Galardi S, Mercatelli N, Giorda E, Massalini S, Frajese GV, Ciafre SA *et al* (2007). miR-221 and miR-222 expression affects the proliferation potential of human prostate carcinoma cell lines by targeting p27Kip1. *J Biol Chem* 282: 23716-23724

Gertsch J, Pertwee RG, Di Marzo V (2010). Phytocannabinoids beyond the Cannabis plant - do they exist? *Br J Pharmacol* 160: 523-529.

Grimaldi P, Orlando P, Di Siena S, Lolicato F, Petrosino S, Bisogno T *et al* (2009). The endocannabinoid system and pivotal role of the CB2 receptor in mouse spermatogenesis. *Proc Natl Acad Sci USA* 106: 11131-11136.

Guindon J, Hohmann AG (2011). The endocannabinoid system and cancer: therapeutic implication. *Br J Pharmacol* 163: 1447-1463.

Gustafsson SB, Lindgren T, Jonsson M, Jacobsson SO (2009). Cannabinoid receptor-independent cytotoxic effects of cannabinoids in human colorectal carcinoma cells: synergism with 5-fluorouracil. *Cancer Chemother Pharmacol* 63: 691-701.

Gutierrez AA, Arias JM, Garcia L, Mas-Oliva J, Guerrero-Hernandez A (1999). Activation of a Ca²⁺-permeable cation channel by two different inducers of apoptosis in a human prostatic cancer cell line. *J Physiol* 517: 95-107.

Hartel A, Didier A, Ulbrich SE, Wierer M, Meyer HH (2004). Characterisation of steroid receptor expression in the human prostate carcinoma cell line 22RV1 and quantification of androgen effects on mRNA regulation of prostate-specific genes. *J Steroid Biochem Mol Biol* 92: 187-197.

Henshall SM, Afar DE, Hiller J, Horvath LG, Quinn DI, Rasiyah KK *et al* (2003). Survival analysis of genome-wide gene expression profiles of prostate cancers identifies new prognostic targets of disease relapse. *Cancer Res* 63: 4196-4203.

Horoszewicz JS, Leong SS, Kawinski E, Karr JP, Rosenthal H, Chu TM *et al* (1983). LNCaP model of human prostatic carcinoma. *Cancer Res* 43: 1809-1818.

Izzo AA, Borrelli F, Capasso R, Di Marzo V, Mechoulam R (2009). Non-psychoactive plant cannabinoids: new therapeutic opportunities from an ancient herb. *Trends Pharmacol Sci* 30: 515-527.

Jacobsson SO, Rongard E, Stridh M, Tiger G, Fowler CJ (2000). Serum-dependent effects of tamoxifen and cannabinoids upon C6 glioma cell viability. *Biochem Pharmacol* 60:1807-1813.

Jacobsson SO, Wallin T, Fowler CJ (2001). Inhibition of rat C6 glioma cell proliferation by endogenous and synthetic cannabinoids. Relative involvement of cannabinoid and vanilloid receptors. *J Pharmacol Exp Ther* 299: 951-959.

Jemal A, Siegel R, Ward E, Hao Y, Xu J, Thun MJ (2009). Cancer statistics, 2009. *CA Cancer J Clin* 59: 225-249.

Kruse JP, Gu W (2009). Modes of p53 regulation. *Cell* 137: 609-622.

Lee SY, Oh SM, Lee SK, Chung KH (2005). Antiestrogenic effects of marijuana smoke condensate and cannabinoid compounds. *Arch Pharm Res* 28: 1365-1375.

Ligresti A, Bisogno T, Matias I, De Petrocellis L, Cascio MG, Cosenza V *et al* (2003). Possible endocannabinoid control of colorectal cancer growth. *Gastroenterology* 125: 677-687.

Ligresti A, Moriello AS, Starowicz K, Matias I, Pisanti S, De Petrocellis L *et al* (2006). Antitumor activity of plant cannabinoids with emphasis on the effect of cannabidiol on human breast carcinoma. *J Pharmacol Exp Ther* 318: 1375-1387.

Lim MP, Devi LA, Rozenfeld R (2011). Cannabidiol causes activated hepatic stellate cell death through a mechanism of endoplasmic reticulum stress-induced apoptosis. *Cell Death Dis* 2: e170.

Maccarrone M, Lorenzon T, Bari M, Melino G, Finazzi-Agrò A (2000). Anandamide induces apoptosis in human cells via vanilloid receptors: evidence for a protective role of cannabinoid receptors. *J Biol Chem* 275: 31938-31945.

Malagarie-Cazenave S, Olea-Herrero N, Vara D, Diaz-Laviada I (2009). Capsaicin, a component of red peppers, induces expression of androgen receptor via PI3K and MAPK pathways in prostate LNCaP cells. *FEBS Lett* 583: 141-147.

Malagarie-Cazenave S, Olea-Herrero N, Vara D, Morell C, Diaz-Laviada I (2011). The vanilloid capsaicin induces IL-6 secretion in prostate PC-3 cancer cells. *Cytokine* 54: 330-337.

Marchiani S, Tamburrino L, Nesi G, Paglierani M, Gelmini S, Orlando C *et al* (2010). Androgen-responsive and -unresponsive prostate cancer cell lines respond differently to stimuli inducing neuroendocrine differentiation. *Int J Androl* 33: 784-793.

Massi P, Vaccani A, Ceruti S, Colombo A, Abbracchio MP, Parolaro D (2004). Antitumor effects of cannabidiol, a nonpsychoactive cannabinoid, on human glioma cell lines. *J Pharmacol Exp Ther* 308: 838-845.

McAllister SD, Murase R, Christian RT, Lau D, Zielinski AJ, Allison J *et al* (2011). Pathways mediating the effects of cannabidiol on the reduction of breast cancer cell proliferation, invasion, and metastasis. *Breast Cancer Res Treat* 129: 37-47.

Melck D, De Petrocellis L, Orlando P, Bisogno T, Laezza C, Bifulco M *et al* (2000). Suppression of nerve growth factor Trk receptors and prolactin receptors by endocannabinoids leads to inhibition of human breast and prostate cancer cell proliferation. *Endocrinology* 141: 118-126.

Mimeault M, Pommery N, Watzet N, Bailly C, Henichart JP (2003). Antiproliferative and apoptotic effects of anandamide in human prostatic cancer cell lines: implication of epidermal growth factor receptor downregulation and ceramide production. *Prostate* 56: 1-12.

Monet M, Lehen'kyi V, Gackiere F, Firlej V, Vandenberghe M, Roudbaraki M *et al* (2010). Role of cationic channel TRPV2 in promoting prostate cancer migration and progression to androgen resistance. *Cancer Res* 70: 1225-1235.

Munson AE, Harris LS, Friedman MA, Dewey WL, Carchman RA (1975). Antineoplastic activity of cannabinoids. *J Natl Cancer Inst* 55: 597-602.

Nomura DK, Lombardi DP, Chang JW, Niessen S, Ward AM, Long JZ *et al* (2011). Monoacylglycerol lipase exerts dual control over endocannabinoid and fatty acid pathways to support prostate cancer. *Chem Biol* 18: 846-856.

Olea-Herrero N, Vara D, Malagarie-Cazenave S, Diaz-Laviada I (2009). Inhibition of human tumour prostate PC-3 cell growth by cannabinoids R(+)-Methanandamide and JWH-015: involvement of CB2. *Br J Cancer* 101: 940-950.

Ortar G, De Petrocellis L, Morera L, Moriello AS, Orlando P, Morera E *et al* (2010). (-)-Menthylamine derivatives as potent and selective antagonists of transient receptor potential melastatin type-8 (TRPM8) channels. *Bioorg Med Chem Lett* 20: 2729-2732.

Ortar G, Ligresti A, De Petrocellis L, Morera E, Di Marzo V (2003). Novel selective and metabolically stable inhibitors of anandamide cellular uptake. *Biochem Pharmacol* 65: 1473-1481.

Papa VM, Shen ML, Ou DW (1990). The effects of pH and temperature on the in vitro bindings of delta-9-tetrahydrocannabinol and other cannabinoids to bovine serum albumin. *J Pharm Biomed Anal.* 8:353-356.

Pfaffl MW (2010). The ongoing evolution of qPCR. *Methods* 50: 215-216.

Portella G, Laezza C, Laccetti P, De Petrocellis L, Di Marzo V, Bifulco M (2003). Inhibitory effects of cannabinoid CB1 receptor stimulation on tumor growth and metastatic spreading: actions on signals involved in angiogenesis and metastasis. *FASEB J* 17:1771-1773.

- Preet A, Ganju RK, Groopman JE (2008). Δ^9 -Tetrahydrocannabinol inhibits epithelial growth factor-induced lung cancer cell migration in vitro as well as its growth and metastasis in vivo. *Oncogene* 27: 339-334
- Qin N, Neeper MP, Liu Y, Hutchinson TL, Lubin ML, Flores CM (2008). TRPV2 is activated by cannabidiol and mediates CGRP release in cultured rat dorsal root ganglion neurons. *J Neurosci* 28: 6231-6238.
- Ramer R, Merkord J, Rohde H, Hinz B (2010). Cannabidiol inhibits cancer cell invasion via upregulation of tissue inhibitor of matrix metalloproteinases-1. *Biochem Pharmacol* 79: 955-966.
- Ren J, Wu JH (2012). 17β -Estradiol rapidly activates calcium release from intracellular stores via the GPR30 pathway and MAPK phosphorylation in osteocyte-like MLO-Y4 cells. *Calcif Tissue Int* (in press)
- Revankar CM, Cimino DF, Sklar LA, Arterburn JB, Prossnitz ER (2005). A transmembrane intracellular estrogen receptor mediates rapid cell signaling. *Science* 307: 1625-1630.
- Robson P (2005) Human studies of cannabinoids and medicinal cannabis. *Handb Exp Pharmacol* 168: 719-756.
- Rokhlin OW, Taghiyev AF, Guseva NV, Glover RA, Chumakov PM, Kravchenko JE *et al* (2005). Androgen regulates apoptosis induced by TNFR family ligands via multiple signaling pathways in LNCaP. *Oncogene* 24: 6773–6784.
- Ruh MF, Taylor JA, Howlett AC, Welshons WV (1997). Failure of cannabinoid compounds to stimulate estrogen receptors. *Biochem Pharmacol* 53: 35-41.
- Ruiz L, Miguel A, Diaz-Laviada I (1999). Δ^9 -tetrahydrocannabinol induces apoptosis in human prostate PC-3 cells via a receptor-independent mechanism. *FEBS Lett* 458: 400-404.
- Russo EB (2011) Taming THC: potential cannabis synergy and phytocannabinoid-terpenoid entourage effects. *Br J Pharmacol* 163: 1344-1364.
- Sanchez C, de Ceballos ML, Gomez del Pulgar T, Rueda D, Corbacho C, Velasco G *et al* (2001). Inhibition of glioma growth in vivo by selective activation of the CB(2) cannabinoid receptor. *Cancer Res* 61:5784-5789.
- Sanchez MG, Sanchez AM, Collado B, Malagarie-Cazenave S, Olea N, Carmena MJ *et al* (2005). Expression of the transient receptor potential vanilloid 1 (TRPV1) in LNCaP and PC-3 prostate cancer cells and in human prostate tissue. *Eur J Pharmacol* 515: 20-27.
- Sanchez AM, Sanchez MG, Malagarie-Cazenave S, Olea N, Diaz-Laviada I (2006). Induction of apoptosis in prostate tumor PC-3 cells and inhibition of xenograft prostate tumor growth by the vanilloid capsaicin. *Apoptosis* 11: 89-99.
- Sarfaraz S, Afaq F, Adhami VM, Mukhtar H (2005). Cannabinoid receptor as a novel target for the treatment of prostate cancer. *Cancer Res* 65: 1635-1641.
- Schiewer MJ, Augello MA, Knudsen KE (2012). The AR dependent cell cycle: Mechanisms and cancer relevance. *Mol Cell Endocrinol* 352: 34-45.
- Shrivastava A, Kuzontkoski PM, Groopman JE, Prasad A (2011). Cannabidiol induces programmed cell death in breast cancer cells by coordinating the cross-talk between apoptosis and autophagy. *Mol Cancer Ther* 10: 1161-1172.
- Torres S, Lorente M, Rodriguez-Fornes F, Hernandez-Tiedra S, Salazar M, Garcia-Taboada E *et al* (2011). A combined preclinical therapy of cannabinoids and temozolomide against glioma *Mol Cancer Ther* 10: 90-103.

Tsavalier L, Shapero MH, Morkowski S, Laus R (2001). Trp-p8, a novel prostate-specific gene, is upregulated in prostate cancer and other malignancies and shares high homology with transient receptor potential calcium channel proteins. *Cancer Res* 61: 3760-3769.

Vaccani A, Massi P, Colombo A, Rubino T, Parolaro D (2005). Cannabidiol inhibits human glioma cell migration through a cannabinoid receptor-independent mechanism. *Br J Pharmacol* 144: 1032–1036.

Valero M, Morenilla-Palao C, Belmonte C, Viana F (2011). Pharmacological and functional properties of TRPM8 channels in prostate tumor cells. *Pflugers Arch* 461: 99-114.

van Bokhoven A, Varella-Garcia M, Korch C, Johannes WU, Smith EE, Miller HL *et al* (2003). Molecular characterization of human prostate carcinoma cell lines. *Prostate* 57: 205-225.

Velasco L, Ruiz L, Sanchez MG, Diaz-Laviada I (2001). Δ^9 -Tetrahydrocannabinol increases nerve growth factor production by prostate PC-3 cells. Involvement of CB1 cannabinoid receptor and Raf-1. *Eur J Biochem* 268: 531-535.

Yu J, Zhang L (2008). PUMA, a potent killer with or without p53. *Oncogene* 27: S71-S83.

Zhang L, Barritt GJ (2004). Evidence that TRPM8 is an androgen-dependent Ca^{2+} channel required for the survival of prostate cancer cells. *Cancer Res* 64: 8365-8373.

Ziglioli F, Frattini A, Maestroni U, Dinale F, Ciufifeda M, Cortellini P (2009). Vanilloid-mediated apoptosis in prostate cancer cells through a TRPV-1 dependent and a TRPV-1-independent mechanism. *Acta Biomed* 80: 13-20.

Legend to Tables and Figures

Table 1: : Effect of plant cannabinoids on the viability of human prostate carcinoma androgen-receptor negative (DU-145) cells. [A]

Cells were seeded in presence of 10%FBS in 6-well Multiwell with a density of 8×10^4 cells/well. After adhesion, cells were treated with increased concentrations of compounds for 72hours (presence of serum was maintained during the treatments). **[B]** Cells were seeded in presence of 10%FBS in 6-well Multiwell with a density of 8×10^4 cells/well. After adhesion, cells were starved for 16h and subsequently treated with increased concentrations of compounds for 24 hours (absence of serum was maintained during the treatments). Cell viability was assessed by MTT staining (see Materials and Methods). Data are reported as mean \pm SD of IC_{50} values calculated from three independent experiments. In the case of $IC_{50} > 25 \mu M$, the maximum inhibition observed at the highest concentration tested (25 μM) is shown.

Table 2: Effect of plant cannabinoids on the viability of human prostate carcinoma androgen-receptor positive (LNCaP) cells. [A]

Cells were seeded in presence of 10%FBS in 6-well Multiwell with a density of 1×10^5 cells/well. After adhesion cells were treated with increased concentrations of compounds for 72hours (presence of serum was maintained during the treatments). **[B]** Cells were seeded in presence of 10%FBS in 6-well Multiwell with a density of 1×10^5 cells/well. After adhesion, cells were starved for 16h and subsequently treated with increased concentrations of compounds for 24 hours (absence of serum was maintained during the treatments). Cell viability was assessed by MTT staining (see Materials and Methods). Data are reported as mean \pm SD of IC_{50} values calculated from three independent experiments. In the case of $IC_{50} > 25 \mu M$, the maximum inhibition observed at the highest concentration tested (25 μM) is shown.

Table 3: Summary of the expression (mRNA expr.) of potential cannabinoid targets and of the cellular and molecular effects of cannabidiol (CBD) observed in this study in the four prostate carcinoma cell lines under investigation. NA, not applicable; NT, not tested.

Figure 1. Serum deprivation or serum content modification differently affect the effect of cannabinoids (CBD, CBG, CBC) on the viability of human PCCs in the MTT assay.

White bars denote DU-145 cells, and black bars denote LNCaP cells. (A) Cells were grown in presence of 10% FBS in 6-well dishes. After adhesion, cells were serum-deprived (with or without 0.5%BSA) for 16h and subsequently treated with compounds for 24 h. Cell viability was assessed by the MTT assay (see Materials and Methods). Data are reported as mean \pm S.E. of % inhibition of MTT reducing activity calculated from three independent experiments. Statistical difference between groups was assessed by ANOVA followed by Bonferroni test [*** $p < 0.001$ FBS-free vs plus 0.5%BSA]. (B) Cells grown in presence of 10% FBS were incubated, after adhesion, under different conditions [a-c] in 6-well dishes for 72 h: [a] cells were incubated in presence of 10% FBS; [b] cells










were incubated with 10% FBS that had been protein-deprived by centrifugation at 3000xg in Centriplus 30kDa centrifugal filter devices; [c] cells were incubated again in 10% FBS that had been protein-deprived as described above, but treated with 0.5%BSA. Cell viability was assessed by the MTT assay (see Methods).

Data are means \pm S.E. of % inhibition of MTT reducing activity calculated from three independent experiments. Statistical differences between groups was assessed by ANOVA followed by Bonferroni test. (### $p < 0.001$ protein-deprived serum [b] vs 10% FBS [a] and protein-deprived serum plus 0.5% BSA [c]; \$\$ $p < 0.01$ protein-deprived serum plus 0.5% BSA [c] vs 10% FBS [a]). (C) Cells were grown in 10% FBS in 6-well dishes. After adhesion, cells were serum-deprived for 16h and then treated with compounds for 24 h. Cell viability was assessed by the MTT assay (see Methods). Data are reported as mean \pm S.E. of % inhibition of MTT reducing activity calculated from three independent experiments.

Figure 2. Effect of CBD-BDS on the growth of xenograft tumors from LNCaP and DU-145 cells in athymic mice, *per se* or co-administered with docetaxel (taxotere) or bicalutamide (casodex). Effect of increasing doses of CBD-BDS (i.p.) or taxotere (i.v.) or combinations thereof, on the growth of LNCaP (A) and DU-145 (B) cell xenografts. See Methods for details. Black squares, vehicle; upward dark red triangles, CBD-BDS 1 mg/kg; down-ward orange triangles, CBD-BDS 10 mg/kg; light green rhombs, CBD-BDS 100 mg/kg; green circles, taxotere 5 mg/kg; blue empty squares CBD-BDS 100 mg/kg plus taxotere 5 mg/kg. N=10 mice were used for each group. In (A) *, $p = 0.0008$; **, $p < 0.0001$ vs. vehicle; ***, $p < 0.0001$ vs. both vehicle and CBD-BDS+taxotere; in (B) *, $p < 0.0001$ vs. vehicle; #, $p < 0.0001$ vs. taxotere alone, calculated using two-way ANOVA. (C) Effect of increasing doses of CBD-BDS (i.p.) or bicalutamide (p.o.) or combinations thereof, on the growth of LNCaP cell xenografts. Also a 50 mg/kg dose of bicalutamide was studied, but the effect was not different from that of the 25 mg/kg dose. * $p = 0.0005$ (Group 5 vs Group 1)* $p = 0.001$ (Group 5 vs Group 2), calculated using two-way ANOVA. (D) Kaplan-Meier survival plots for the study described in (C). Statistical significance was assessed by using the Log Rank-Wilcoxon analysis.

Figure 3. Effect of cannabinoids and on the release of caspase 3/7 from various PCC lines. Cells (10,000 per data point) were treated under the conditions shown and caspase 3/7 activity was assessed with the luminescence assay described in the Methods. Other compounds tested that exhibited no activity are not shown. Effect of various compounds, at various concentrations, in LNCaP (A) and DU-145 (DU) (B) cells incubated in the presence of serum for 24 h, and of the positive control, anti-FAS+camptothecin (campto+AFAS). Note how the TRPM8 antagonist OMDM233 stimulates release and how the TRPM8 agonist icilin inhibits the effect of CBD in LNCaP cells. (C) Effect of varying duration of serum deprivation (SDP) before and after treatment (12 h + 8 h treatment, 12 h + 12 h treatment, 24 h + 12 h treatment) with varying doses of the TRPM8 antagonist OMDM233, or of the TRPM8 agonist icilin, or of CBD, with and without icilin, on caspase 3/7 activity in LNCaP cells. (D) Effect of various durations of SDP before and after

treatment (12 h + 12 h treatment, 12h + 24 h of treatment, or 24 h + 12 h treatment) with varying doses of CBG and CBC on caspase 3/7 activity in LNCaP cells. (E) Effect of BSA (0.5%), or testosterone (T, 50 μ M), or subsequent addition of FBS, or of the use of charcoal-stripped FBS (strip) on the effect of CBD on caspase 3/7 activity in LNCaP cells. These experiments were carried out under different conditions of pre-treatment serum-deprivation (12 or 24 h), whereas the treatment with CBD (10 μ M) was always carried out for 12 h, thus leading to total durations of experiments of 24 or 36 h. (F) Effect of CBD on caspase 3/7 activity in SDP DU-145 cells. Experiments were carried out with either varying doses of CBD for 18 h, after a previous serum deprivation of 6 h, or with 10 μ M CBD for a total of 24 h with different combinations of previous serum deprivation (0, 2 and 4 h) and treatment (24, 22 and 20 h). Finally, the effect of CBC and CBG were studied in 22RV1 (G) and PC3 (H) cells. In both cases the experiment lasted for 24 h, with a previous serum deprivation of 4h in (G) and 6h in (H). Data are means \pm S.E. of at least n=3 experiments. Means were compared by ANOVA followed by the Bonferroni test. *, p<0.05; **, p<0.01; ***, p<0.001 vs. respective control (first bar in each panel, which represents the baseline level of caspase 3/7, which, for a given cell line, did not vary significantly regardless of the duration of the experiment and the presence of serum in the 12-36h range). In (C,E) #, p<0.01 vs. SDP 24 + 12 CBD 10 μ M.

Figure 4. Molecular mechanisms of the pro-apoptotic effect of CBD in prostate carcinoma cells. (A) Effect of CBD (10 μ M) on the mRNA expression of the p53-upregulated modulator of apoptosis (PUMA) in the four PCC lines examined in this study. Cells were cultured in presence of serum , in serum deprived medium  for 24 hrs and in presence of 10 μ M CBD  in the optimal conditions evaluated by caspase 3/7 assay, ie: 12h (LNCaP), 18 h (DU-145 and PC3) and 20 h (22RV1) of CBD treatment after 12, 6 and 4 h of previous serum-deprivation, respectively. The expression levels, normalized respect to reference genes, were scaled for each cell line to the expression value of the cells cultured in presence of serum, put as 1. The means of the quantitative-cycles (cq) for the these conditions were: 28.68 (LNCaP), 28.62 (DU-145), 27.32 (PC3) and 25.63 (22RV1). The reaction background was 37.30 cq. (B) Representative western blots for the stimulatory effect of CBD on the expression and phosphorylation of p53 in LNCaP, DU-145 and 22RV1 cells, serum-deprived for 12 h and then treated with vehicle or CBD (10 μ M) for a further 12 h. Histograms show the quantitative determination of the chemoluminescence in western blots from two separate experiments, normalized to β -actin, and expressed as fold-amounts relative to the corresponding serum-deprived, vehicle-treated control cells.  LNCaP,  22RV1 and  DU-145 cells. (C) Transcriptional expression of CHOP in prostatic cell lines: CHOP mRNA levels in LNCaP, DU-145, PC3 and 22RV1 prostatic cancer cell lines. Cell were cultured in presence of serum , in serum deprived medium  for 24 hrs and in presence of 10 μ M CBD  in the optimal conditions evaluated by caspase 3/7

assay, (see [A]). qRT-PCR was performed as described in *Methods*, using 20 ng of cDNA/assay. The expression levels, normalized respect to reference genes, were scaled for each cell-line to the expression value of the cells cultured in presence of serum, put as 1. The means of quantitative-cycles (cq) for the these conditions were: 24.88cq (LNCaP), 20.73cq (DU-145), 21,79cq (PC3) and 21,87cq (22RV1). The reaction background was 35.30 cq. Standard deviations were calculated by the Gene expression module of iQ5 real-time PCR. All differences indicated in the graph with (*) were statistically significant ($P < 0.05$) as evaluated according to Pfaffl et al. 2010 (See Supplementary Materials). A typical experiment (R.I.N. > 8.5, see *Methods*) is shown. (D, E) LNCaP cells were cultured in presence of serum (CTR), in serum deprived medium for 24 h (SDP), and in presence of 10 μ M CBD for 12 (LNCaP cells) or 20 (22RV1) h during 24 h total growth in serum deprived medium (SDP+CBD). LNCaP cells (D) were also growth for 24 h in serum deprived medium containing testosterone 50 μ M in absence (SDP+T) or in presence (SDP+T+CBD) of CBD, following the conditions described above. The expression levels normalized respect to the reference gene were scaled to the lowest expression value condition (i.e. SDP+T+CBD, 26.76 cq vs background > 40 cq for [D], and CTR, 26.76 cq vs background > 40 cq, for [E]), considered as 1. (F) LNCaP cells were cultured in presence of serum (CTR), in serum deprived medium for 24 h (SDP) and in presence of 10 μ M CBD for 12 h during 24 h total growth in serum deprived 50 μ M in absence (SDP+T) or in presence (SDP+T+CBD) of CBD, following the conditions described above. The expression levels normalized respect to the reference gene, were scaled to the lowest expression value condition (SDP, 27.30 cq vs background at 35.01 cq), considered as 1. In (A,C,D,E) a representative experiment (R.I.N. > 8.5, see *Methods*) is shown and qRT-PCR was performed as described in *Methods*, using 20 ng of cDNA/assay. Standard deviations were calculated by the Gene expression module of iQ5 real-time PCR. All differences indicated in the graph (*) were significant ($p < 0.05$ vs. values in dark grey bars) as evaluated according to Pfaffl *et al.* 2010 (See Supplementary Materials). In (F) # denotes $p < 0.05$ vs. SDP and § denotes $p < 0.05$ vs. SDP+T.









Figure 5. Effect of cannabinoids on intracellular Ca^{2+} and reactive oxygen species (ROS) in prostate carcinoma cells. (A) Typical dose-dependent effects for cannabinoids on intracellular Ca^{2+} in PCCs, with either efficacy or potency being higher in cells serum-deprived (SDP) for 24 h. The effect of CBG in LNCaP and DU-145 cells is shown. See Supplementary Table 6 for the full data in the four PCCs with CBD, CBG and CBC. (B,C) Involvement of ROS in the effect of CBD on different PCCs. Time course of ROS production by PCC cells as measured by spectrofluorometric analysis as described in *Methods*. Fluorescence detection was carried out after the incubation of either 100 μ M H_2O_2 or CBD (10 μ M) at different times (0–30–60–120 min) in cells grown in normal medium (B) or in cells kept without serum prior to treatment (C). The fluorescence measured at time 0 was considered as basal ROS production and subtracted from the fluorescence at different times ($\Delta 1$). Data are reported as $\Delta 2$, i.e., $\Delta 1$ values at different doses subtracted of the $\Delta 1$ values of cells incubated with vehicle, and are mean \pm S.E. of at least $n = 3$ experiments. Note how

the effect of both CBD (red bars) and H₂O₂ (black bars) becomes significant only in the absence of serum (C) and only in LNCaP cells.

Figure 6. Effects of CBD on neuroendocrine-like LNCaP cells. Cells were differentiated with dbcAMP+IBMX for 36 h in serum deprived medium, as described in Methods, in the presence or absence of CBD and various other compounds. (A) Effect on caspase 3/7 activity of just serum deprivation for 36 h, alone or with CBD (10 μM) for 12 h, or with dbcAMP+IBMX for 36 h, or with dbcAMP+IBMX for 24 h followed by 12 h CBD, or with dbcAMP+IBMX followed by 12 h icilin (1 μM) or OMDM233 (2 μM), or with dbcAMP+IBMX followed by 12 h CBD+ icilin. *, **, ***; p<0.05, 0.01, 0.001 vs. SDP 36. (B) neuron-specific enolase (NSE) mRNA in differentiated LNCaP cells. Cells were cultured in the presence of serum (CTR), in serum deprived medium for 36 h in the presence of dbcAMP and IBMX (dbcAMP) and in presence of 10 μM CBD for 12 hrs during dbcAMP + IBMX treatment (dbcAMP+CBD). qRT-PCR was performed as described in Methods using 20 ng of cDNA/assay. The expression levels of NSE mRNA, normalized respect to the reference gene, were scaled to the lowest expression value condition, put as 1, ie: dbcAMP+CBD (28,67 cq vs background > 40cq). PUMA (C), p27 kip (D), AR (E) and TRPM8 (F) mRNA levels in LNCaP cells following various treatments in serum deprived (SDP) cells. Cell were cultured in presence of serum (CTR), in serum deprived medium for 36 h in presence of dbcAMP + IBMX (dbcAMP) and in presence of 10 μM CBD for 12 h during dbcAMP + IBMX treatment (dbcAMP+CBD). For all the targets, the expression levels normalized respect to the reference gene, were scaled to the lowest expression value condition, put as 1, ie: CTR (28.68 cq vs background at 37.53) for PUMA and p^{27kip} (24.75 cq vs background > 38,40cq); and dbcAMP+CBD for AR (29.04 vs background >40cq) and TRPM8 (29.50 vs background at 35.80 cq). In (B-F) qRT-PCR was performed as described in Methods using 20 ng of cDNA/assay, and a typical experiment (R.I.N. > 8.5, see Methods) is depicted. Standard deviations were calculated by the Gene expression module of iQ5 real-time PCR. All differences indicated in the graph (*) were significant (P < 0.05) vs. CTR as evaluated according to Pfaffl et al. 2010 (See Supplementary Materials). # denotes p<0.05 vs. dbcAMP.

Legends to Supplementary Figures and Tables

Supplementary Figure 1. Transcriptional expression of TRP channels and cannabinoid receptors in

prostatic cancer cell lines. (A) TRPV1, TRPV2, TRPM8 and TRPA1 mRNA levels in  LNCaP,  DU-145,  PC3 and  22RV1 cells. The means of quantitative-cycles (cq) for the highest expression values were 26.25 for TRPV1 (DU-145), 31.13 for TRPV2 (DU-145), 26.22 for TRPM8 (LNCaP) and 26.50 for TRPA1 (DU). For all targets, the expression levels normalized respect to the reference gene, were scaled to the lowest expression value, considered as 1. These were: LNCaP for TRPV1 (31.70 cq vs background at 37.53 cq), TRPV2 and TRPA1 (for both the targets the expression levels were coincident to background at 35.64 and 37.30 cq, respectively); and 22RV1 for TRPM8 (expression level close to background 33.05 vs 34.80 cq). qRT-PCR was performed as described in Methods using 20 ng of cDNA/assay. Standard deviations were calculated by the Gene expression module of iQ5 real-time PCR. All differences indicated in the graph (*) were significant ($P < 0.05$) as evaluated according to Pfaffl et al. (2010). A typical experiment (R.I.N. > 8.5, see Methods) is depicted for each gene. (B) CB1 and CB2 mRNA levels  LNCaP,  DU-145,  PC3 and  22RV1 cells. The means of quantitative-cycles (cq) for the higher expression values were 27.53 for CB1 (PC3) and 27.44 for CB2 (PC3). For both targets, the expression levels normalized respect to the reference gene, were scaled to the lowest expression value, put as 1. These were: DU-145 for CB1 (expression level close to background 35.87 vs 37.25 cq), and 22RV1 for CB2 (expression level close to background 35.34 vs 36.9 cq). qRT-PCR was performed as described in Methods using 20 ng of cDNA/assay. Standard deviations were calculated by the Gene expression module of iQ5 real-time PCR. A typical experiment (R.I.N. > 8.5, see Methods) is depicted for each gene. (C) Representative western blot analysis of TRPM8 in LNCaP cells grown in serum-containing medium (CTR) and in medium deprived of serum for 36 h (SDP).

Supplementary Figure 2. Effect of cannabinoid receptor or TRP channel agonists and antagonists on PCC

viability in MTT assays. White bars denote DU-145 cells, and black bars denote LNCaP cells. (A) After adhesion, cells were treated with compounds for 72 h [Capsaicin abbreviated as CPS; Resiniferatoxin abbreviated as RTX]. These effects were not antagonized by the selective TRPV1 antagonist, I-RTX (not shown). Only the effects of capsaicin 25 or 50 μ M (in LNCaP and DU-145 cells, respectively) reached statistical significance ($p < 0.05$, ANOVA followed by Bonferroni's test). (B) After adhesion, cells were treated with Allylisothiocyanate (abbreviated as MO) an agonist of TRPA1 receptor for 72 h. Only the effects of MO reached statistical significance ($p < 0.05$, ANOVA followed by Bonferroni's test), and were not antagonized by the two selective TRPA1 antagonists, HC030031 and AP18. (C) After adhesion, cells were treated with selective agonist (Icilin) and antagonist (OMDM 233) of TRPM8 channels for 72 h. Only the

effects of Icilin 2 μ M, and OMDM233 1 and 10 μ M reached statistical significance, and only in LNCaP cells ($p < 0.05$, ANOVA followed by Bonferroni's test), (D) After adhesion, cells were treated with agonists and /or antagonists of CB receptors for 72 hours [HU-210 was used at 10 μ M; WIN55.212-2 (abbreviated as WIN) was used at 10 μ M; SR141716A (abbreviated as SR1) was used at 0.5 μ M; SR144528 (abbreviated as SR2) was used at 0.5 μ M]. Only the effects of WIN and HU reached statistical significance ($p < 0.05$, ANOVA followed by Bonferroni's test). In (A-D) Data are means \pm S.E. of % inhibition of MTT reducing activity calculated from three independent experiments. Cells were treated the in presence of 10% FBS in 6-well dishes, but similar results were obtained in serum deprived medium (not shown).

Supplementary Figure 3. Interactions between cannabidiol and standard chemotherapics on PCC viability in MTT assays. LNCaP (A) or DU-145 (C) cells were grown in presence of 10% FBS in 6-well dishes. After adhesion, cells were treated with increasing concentrations of docetaxel tested both in the presence and absence of different concentrations of CBD for 72 h at the doses shown. (B) LNCaP cells were grown in presence of 10% FBS in 6-well dishes. After adhesion, cells were treated with a suboptimal concentration of bicalutamide both in presence (MIX) and absence of CBD for 72 h. Dotted line indicates the algebraic sum of the effects of bicalutamide and CBD per se. In (A,B), data are reported as mean \pm S.E. of % inhibition of MTT reducing activity calculated from three independent experiments.




Supplementary Figure 4. Effect of cannabinoid BDS and on the release of caspase 3/7 from various PCC lines. Cells (10,000 per data point) were treated in the presence of serum for 24 h and caspase 3/7 activity was assessed with the luminescence assay described in the Methods. Other BDS tested that exhibited no activity are not shown. Effect of various BDS, at various concentrations, in LNCaP (A) and DU-145 (B) cells. Data are means \pm S.E. of at least $n=3$ experiments. Means were compared by ANOVA followed by the Bonferroni test. *, $p < 0.05$ vs. respective control (first bar in each panel).

Supplementary Figure 5. Dose- and time-dependent effects of CBD on the release of caspase 3/7 from LNCaP cells. Cells (10,000 per data point) were treated with CBD (1, 5 or 10 μ M) under the conditions shown in the absence of serum (SDP), and caspase 3/7 activity was assessed with the luminescence assay described in the Methods. The number near "SDP" refers to the hours of serum deprivation prior to incubation with CBD, which was carried out for the hours shown near "CBD". Data are means \pm S.E. of at least $n=3$ experiments. Means were compared by ANOVA followed by the Bonferroni test. *, $p < 0.05$; **, $p < 0.01$; ***, $p < 0.001$ vs. respective control (LNCaP, vehicle for 24 h). The control levels of caspase 3/7 did not vary significantly regardless of the duration of the experiment in the 9-48h range.

Supplementary Figure 6. Effect of antagonists on CBD-induced release of caspase 3/7 from LNCaP cells. Cells (10,000 per data point) were treated with CBD (10 μ M) for 12 h after 24 h of serum deprivation (SDP)

in the presence of absence of the CB1 antagonist, SR141716A (SR1, 0.5 μ M), or the CB2 antagonist, SR144528 (SR2, 0.5 μ M), or the TRPV1 antagonist iodo-resiniferatoxin (IRTX, 0.2 μ M), and caspase 3/7 activity was assessed with the luminescence assay described in the Methods. Data are means \pm S.E. of at least n=3 experiments. No statistically significant differences were observed towards serum-deprived cells incubated for 36 h with vehicle.

Supplementary Figure 7. Effect of cannabinoids on caspase 3/7 release from DU-145 cells. Cells (10,000 per data point) were treated with CBD (10 μ M), CBC (20 μ M) or CBG (20 μ M) for 18 h in the absence of serum and after 8 h of serum deprivation (SDP), for a total duration of the experiment of 24 h. Data are means \pm S.E. of at least n=3 experiments. Means were compared by ANOVA followed by the Bonferroni test. *, p<0.05; **, p<0.01; ***, p<0.001 vs. SDP.

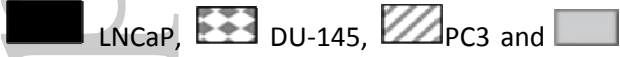
Supplementary Figure 8. Pro-apoptotic effects of CBD in LNCaP cells. (A-D) Pro-apoptotic effects of CBD in PCC cells, evaluated by TUNEL assay. The number of TUNEL-positive cells was evaluated by a Lab-on Chip approach using a Bioanalyzer (Agilent), as described in Methods. [A] LNCaP, [B] DU-145, [C] PC3 and [D] 22RV1 prostate cancer cells were grown in absence of serum for 24 hrs (SPD, left panels). For CBD treatment, the cells were grown in SDP for 12h (LNCaP), 6h (DU-145 and PC3) and 4h (22RV1) and then treated with CBD (10 μ M) for further 12h (LNCaP), 18h (DU-145 and PC3) and 20h (22RV1) in SDP (right panels). At the indicated times, vehicle was added to SDP conditions (see also Supplementary Table 4 for quantitative data relative to the panels). (E, F) Evaluation of cell cycle by FACS scan analysis. LNCaP (E) and DU-145 (F) cells were cultured and treated with CBD (10 μ M) as described for panels A-D. Cell cycle analysis was performed as described in Methods (see Supplementary Tables 5,6 for quantification of these analyses). (G) p27^{kip} mRNA levels in PCC cells. Cells were cultured in the presence of serum , in serum deprived medium  for 24 hrs and treated with 10 μ M CBD  as described for panels A-D (see above). The expression levels normalized to the reference gene, were scaled for each cell line to the expression value of the cells cultured in SDP, considered as 1. The means of quantitative-cycles (cq) for these conditions were: 24.75 cq (LNCaP), 23.90 cq (DU-145), 25.91 cq (PC3) and 24.71 cq (22RV1). The reaction background was 38.04 cq. A representative experiment (R.I.N. > 8.5, see Methods) is depicted and qRT-PCR was performed as described in Methods, using 20 ng of cDNA/assay. Standard deviations were calculated by the Gene expression module of iQ5 real-time PCR. All differences indicated in the graph (*) were significant (p < 0.05 vs. values in dark grey bars) as evaluated according to Pfaffl *et al.* (2010).

Supplementary Figure 9. TUNEL and TRPM8 immunofluorescence in LNCaP and DU-145 cells. Representative images of differentially interference contrasted DU-145 (A,B) and LNCaP (C-F) cells. (A-E) Double staining for TRPM8 immunoreactivity (red) and TUNEL labeling (green) after serum deprivation with

or without (-S) CBD treatment in DU-145 (A,B) and LNCaP (C,D) cells. Note the TRPM8 expression in LNCaP (C-E), but not in DU-145 (A,B), cells and the increase of the number of TUNEL-positive cells in LNCaP and DU-145 cell lines after CBD treatment compared to starvation. The specificity of CBD-induced TUNEL immunofluorescence was shown in LNCaP cells incubated with the TUNEL label solution in absence of the enzyme terminal deoxynucleotidyl transferase (E). (F) Co-localization of TRPM8 and calnexin expression (yellow signal) in TRPM8/Calnexin/DAPI merged image. Scale bar=10 μ m.

Supplementary Figure 10. DNA fragmentation pro-apoptotic effect of CBD in LNCaP cells. Apoptotic fragmentation pattern was evaluated as described in Methods by lab-on-chip technology. Electropherogram profiles showing a typical DNA fragmentation pattern in LNCaP cells growth in serum-deprived medium for a total of 24 h in the presence of vehicle (lower trace in [A]) or 10 μ M CBD (lower trace in [B]) for 12 h. In both A and B the electropherogram (dark-grey) of a positive control (Jurkat cells treated for 4 h with anti-fas plus camptothecin) was superimposed for a comparison. Insets: gel-like images of electrophoretic profiles of vehicle and CBD-treated cells.

Supplementary Figure 11. LNCaP differentiation into neuroendocrine-like cells. Light microscope photo of LNCaP cells incubated with medium + serum for up to 72 h (upper panel, CTR), with medium without serum for 72 h (middle panel), or with dbcAMP plus IBMX for 36 h (lower panel). Note the neurite-like structures in the middle and lower panels.

Supplementary Figure 12. Role of estradiol and estrogen receptors in the pro-apoptotic effects of cannabidiol. (A) Effect of 17 β -estradiol (10 μ M), per se or given together with CBD (10 μ M), on the release of caspase 3/7 in LNCaP cells (10,000 cells per data point), treated under the conditions shown. Caspase 3/7 activity was assessed with the luminescence assay described in the Methods; (B) GPER mRNA levels in  LNCaP, DU-145, PC3 and 22RV1 cells. The means of quantitative-cycles (cq) for the highest expression values were 24.60 (LNCaP). For all targets, the expression levels normalized respect to the reference gene, were scaled to the lowest expression value, considered as 1 (27,21 cq, DU-145). The background was > 40 cq. qRT-PCR was performed as described in Methods using 20 ng of cDNA/assay. Standard deviations were calculated by the Gene expression module of iQ5 real-time PCR. All differences indicated in the graph (*) were significant ($P < 0.05$) as evaluated according to Pfaffl *et al.* (2010). A typical experiment (R.I.N. > 8.5, see Methods) is depicted; (C) effect of the GPER antagonist, G15, on the release of caspase 3/7 in LNCaP cells (10,000 cells per data point) treated under the conditions shown; (D) Calcium release from intracellular stores: dose-dependent effects of G15 on CBD 10 μ M-induced Fura-2 fluorescence. Conditions are described in Supplementary Table 7. In (C) *= $P < 0.05$ vs. SDP+CBD; in (D) *, $P < 0.05$; **, $P < 0.01$ vs. CBD.

Supplementary Table 1 : Sequences of the q-PCR primers used in this study. Primer sequences and temperature-optimum-annealing (TaOpt) were designed as described in Methods. In parentheses, column 1, the target gene acronyms used in the text are shown.

Supplementary Table 2: Effect of plant cannabinoids on the viability of human prostate carcinoma androgen-receptor negative (PC-3) cells. [A] Cells were seeded in presence of 10%FBS in 6-well Multiwell with a density of 6×10^4 cells/well. After adhesion cells were treated with increased concentrations of compounds for 72hours (presence of serum was maintained during the treatments). [B] Cells were seeded in presence of 10%FBS in 6-well Multiwell with a density of 6×10^4 cells/well. After adhesion, cells were starved for 16h and subsequently treated with increased concentrations of compounds for 24 hours (absence of serum was maintained during the treatments). Cell viability was assessed by MTT staining (see Materials and Methods). Data are reported as mean \pm SD of IC₅₀ values calculated from three independent experiments. In the case of IC₅₀>25 μ M, the maximum inhibition observed at the highest concentration tested (25 μ M) is shown.

Supplementary Table 3: Effect of plant cannabinoids on the viability of human prostate carcinoma androgen-receptor positive (22RV1) cells. [A] Cells were seeded in presence of 10%FBS in 6-well Multiwell with a density of 6×10^4 cells/well. After adhesion cells were treated with increased concentrations of compounds for 72hours (presence of serum was maintained during the treatments). [B] Cells were seeded in presence of 10%FBS in 6-well Multiwell with a density of 6×10^4 cells/well. After adhesion, cells were starved for 16h and subsequently treated with increased concentrations of compounds for 24 hours (absence of serum was maintained during the treatments). Cell viability was assessed by MTT staining (see Materials and Methods). Data are reported as mean \pm SD of IC₅₀ values calculated from three independent experiments. In the case of IC₅₀>25 μ M, the maximum inhibition observed at the highest concentration tested (25 μ M) is shown.

Supplementary Table 4: Pro-apoptotic effects of CBD in PCC cells evaluated by TUNEL assay (Lab-on Chip approach, see also Supplementary fig 8). Quantitative data relative to Supplementary Fig 8 (panel A-D). Data are expressed as the mean \pm SD from two independent experiments carried out in cells serum-deprived (SDP) for 24h (of which 18 h of incubation with either vehicle or CBD, 10 μ M). Jurkat cells, treated for 4h with camptothecin and anti-Fas, were used as positive apoptotic control (18.5 \pm 2.0 vs 4.0 \pm 1.9 for untreated control).

Supplementary Table 5: Effect of cannabidiol (CBD) on LNCaP cell cycle as assessed by FACS scan. Quantitative data relative to Supplementary Fig 8 (panel E). Population analysis (%) of LNCaP cells kept for 24 h with vehicle in a serum-containing medium, or kept for 12 h without serum plus 12 h treatment with

either vehicle (SDP) or CBD, 10 μ M, in serum deprived medium (SDP+CBD). Data represent the means \pm SD of two experiments.

Supplementary Table 6: Effect of cannabidiol (CBD) on DU-145 cell cycle as assessed by FACS scan.

Quantitative data relative to Supplementary Fig 8 (panel F). Population analysis (%) of DU-145 cells kept for 24 h with vehicle in a serum-containing medium, or kept for 6 h without serum plus 18 h treatment with either vehicle (SDP) or CBD, 10 μ M, in serum deprived medium (SDP+CBD). Data represent the means \pm SD of two experiments.

Supplementary Table 7: Effect of cannabinoids on intracellular Ca^{2+} in prostatic cancer cell lines. The efficacies, as % of the maximum effect determined in each experiment with ionomycin (4 mM), and potencies, as EC_{50} , of cannabidiol (CBD), cannabichromene (CBC) and cannabigerol (CBG), are shown and as means \pm SD of three experiments, carried out either in cells grown in serum-containing medium or in cells serum deprived for 24 h (SDP). *, $P < 0.05$ vs. the corresponding control (non-SDP data), assessed by ANOVA followed by the Bonferroni's test.

Supplementary Table 8: Expression of oestrogen receptors $ER\alpha$ and $ER\beta$ in LNCaP cells. qRT-PCR analysis was performed as described in Materials and Methods. In LNCaP cells $ER\alpha$ mRNA resulted undetectable; $ER\beta$ Relative Normalized mRNA Expression was about 12 fold lower than mRNA expression observed in MCF7 human breast carcinoma cells, which were considered as 1 when calculating the relative quantity, and also used as positive control. * RNA polymerase II subunit (RNA pol) was used as reference gene. Cq, threshold cycles.

Supplementary Table 9: Chemical composition of Cannabis enriched extracts used in this study. For each Botanical Drug Substance (BDS), the percentage of the main cannabinoid content as well as of the other cannabinoids (w/w) are provided.

PURE COMPOUND	IC₅₀ on cell vitality [A]	IC₅₀ on cell vitality [B]	Botanical drug substances	IC₅₀ on cell vitality [A]	IC₅₀ on cell vitality [B]
CBD	25.3 ± 8μM	5.4 ± 1μM	CBD BDS	9.0 ± 4μM	7.8 ± 2μM
CBC	>25μM (40.7%)	8.5 ± 3μM	CBC BDS	9.2 ± 3μM	7.9 ± 1μM
CBG	>25μM (17.3%)	10.4 ± 1μM	CBG BDS	10.4 ± 5μM	6.9 ± 2μM
CBDV	21.0 ± 4μM	20.0 ± 5μM	CBDV BDS	17.1 ± 7μM	10.3 ± 1μM
THCV	>25μM (38.6%)	20.5 ± 3μM	THCV BDS	>25μM (41.0%)	8.3 ± 1μM
THCVA	>25μM (25.6%)	>25μM (36.1%)	THCVA BDS	>25μM (30.9%)	12.4 ± 1μM
THCA	>25μM (21.9%)	21.6 ± 2μM	THCA BDS	18.9 ± 2μM	9.9 ± 2μM
CBDA	>25μM (11.2%)	10.9 ± 4μM	CBDA BDS	>25μM (27.8%)	15.9 ± 2μM
CBGA	>25μM (7.7%)	11.2 ± 2μM	CBGA BDS	19.2 ± 2μM	12.3 ± 3μM
CBGV	>25μM (11.3%)	>25μM (23.3%)	CBGV BDS	>25μM (21.9%)	10.2 ± 2μM
CBN	>25μM (17.2%)	>25μM (21.8%)	-	-	-
THC	>25μM (6.6%)	11.7 ± 3μM	-	-	-

Table 1

PURE COMPOUND	IC₅₀ on cell vitality [A]	IC₅₀ on cell vitality [B]	Botanical drug substances	IC₅₀ on cell vitality [A]	IC₅₀ on cell vitality [B]
CBD	25.0 ± 3μM	5.7 ± 2μM	CBD BDS	18.1 ± 6μM	6.6 ± 2μM
CBC	20.0 ± 5μM	10.9 ± 3μM	CBC BDS	>25μM (25.6%)	7.9 ± 1μM
CBG	>25μM (34.5%)	11.2 ± 4μM	CBG BDS	21 ± 8μM	9.0 ± 1μM
CBDV	>25μM (27.6%)	20.0 ± 3μM	CBDV BDS	>25μM (24.4%)	10.4 ± 1μM
THCV	>25μM (28.5%)	17.5 ± 3μM	THCV BDS	16.3 ± 5μM	7.2 ± 1μM
THCVA	>25μM (32.4%)	11.5 ± 5μM	THCVA BDS	19.4 ± 8μM	5.6 ± 1μM
THCA	22.1 ± 2μM	17.1 ± 1μM	THCA BDS	15.0 ± 2μM	4.0 ± 3μM
CBDA	>25μM (30.2%)	16.2 ± 5μM	CBDA BDS	>25μM (34.5%)	9.3 ± 2μM
CBGA	>25μM (7.0%)	11.6 ± 2μM	CBGA BDS	14.5 ± 2μM	8.5 ± 2μM
CBGV	>25μM (23.9%)	>25μM (41.0%)	CBGV BDS	>25μM (40.2%)	9.4 ± 2μM
CBN	14.5 ± 6μM	>25μM (34.2%)	-	-	-
THC	16.9 ± 3μM	5.5 ± 3μM	-	-	-

Table 2

Table 3

Cell line	AR mRNA expr.	CB1 mRNA expr.	CB2 mRNA expr.	TRPV1 mRNA expr.	TRPM8 mRNA expr.	CBD effect on cell cycle markers (p21, p27 ^{kip} , G1-S phase transition)	CBD effect on apoptosis	CBD effect on PUMA expression	CBD effect on p53 phosphorylation vs. expression	CBD effect on CHOP expression	CBD effect on [Ca ²⁺] _i	CBD inhibition of AR expression	Effect of TRPM8 agonism on CBD proapoptotic action	Effect of GPER antagonism on CBD proapoptotic action
LNCaP	+++	+	+	+	+++	++	+++	+++	+	++++	+++	++	+	+
22RV1	++	+	-	++	-	++	++	+++	-	++	++	+	NA	NT
DU-145	-	-	+	+++	-	+++	+++	+++	-	+	+	NA	NA	NT
PC-3	-	++++	++++	+	+	+	++	+++	p53 is not expressed	+++	++	NA	NA	NT

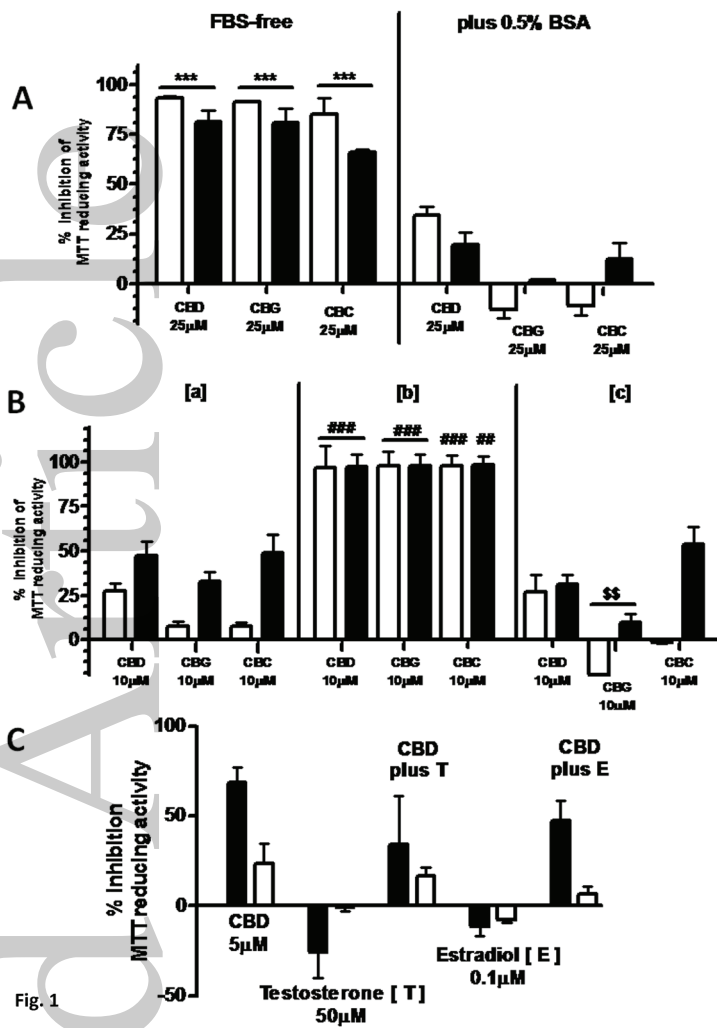


Fig. 1

Accepted Article

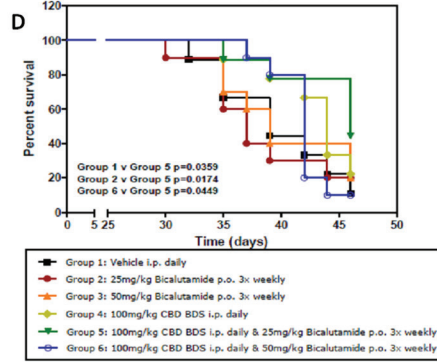
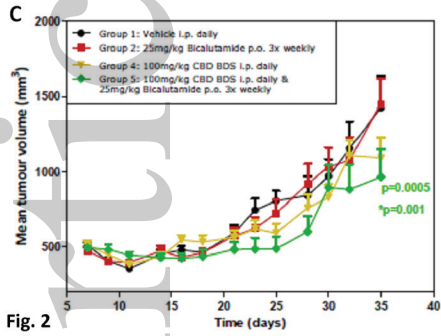
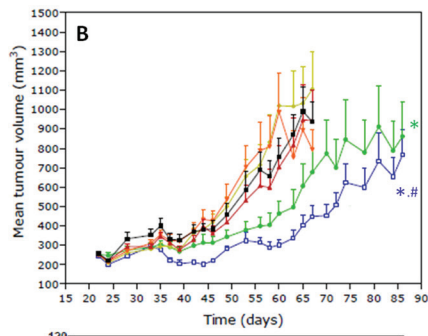
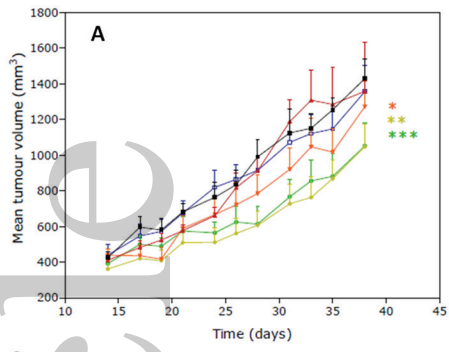


Fig. 2

Accepted Article

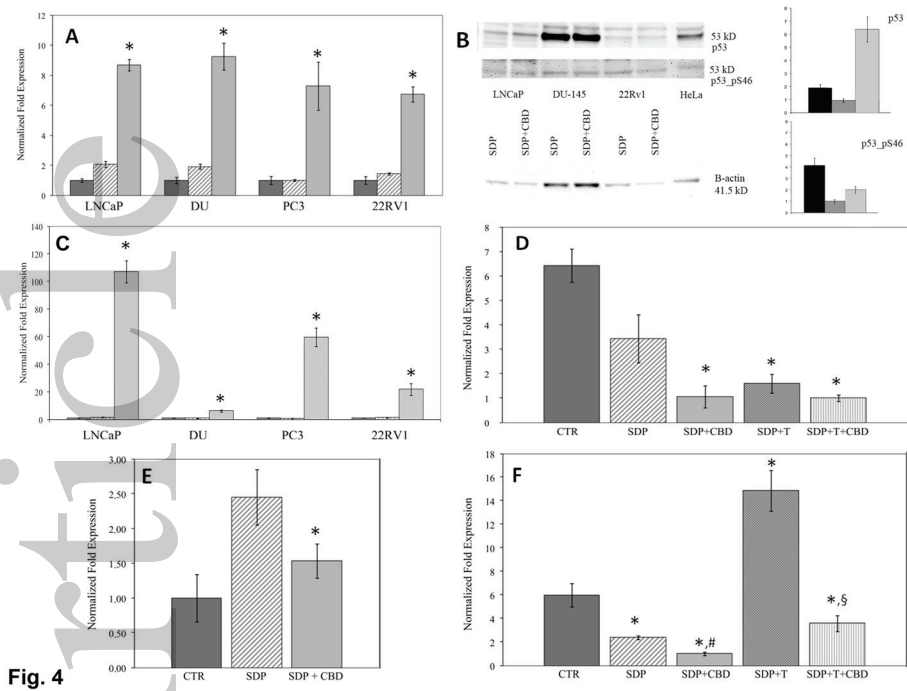


Fig. 4

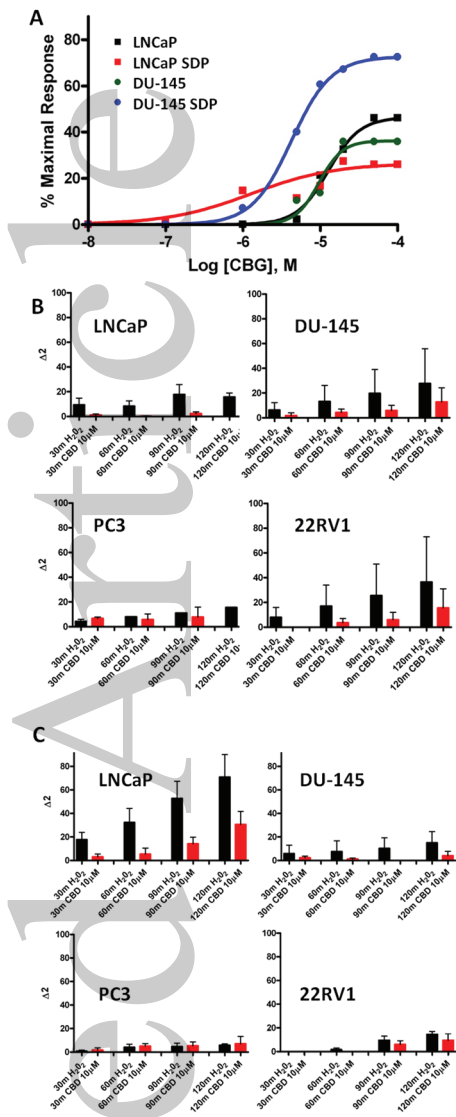


Fig. 5

ACCEPTED MANUSCRIPT

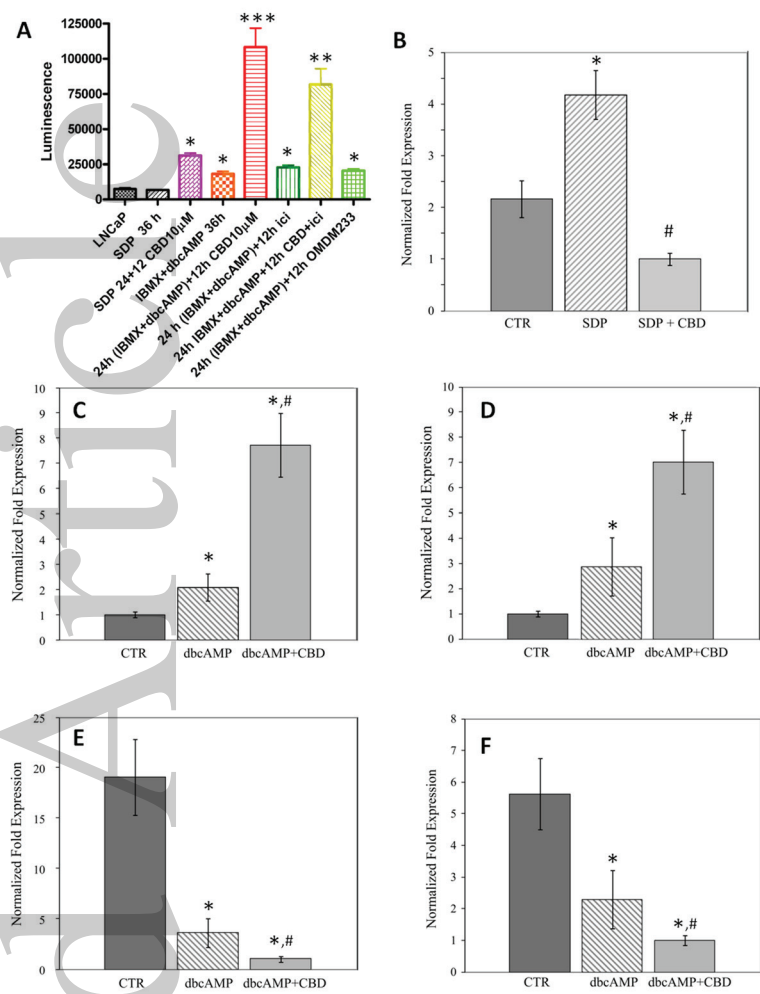


Fig. 6

Accepted Article